The role of *C. elegans* NHR-49 in regulating global lipid homeostasis

Pranali Pathare

A dissertation submitted in partial fulfillment of the
requirements for the degree of

Doctor of Philosophy

University of Washington

2011

Program Authorized to Offer Degree:
Molecular and Cellular Biology

University of Washington
Graduate School

This is to certify that I have examined this copy of a doctoral dissertation by

Pranali Pathare

and have found that it is complete and satisfactory in all respects,
and that any or all revisions required by the final
examining committee have been made.

Chair of the Supervisory Committee:

Susan Biggins

Reading Committee:

Susan Biggins

Susan Biggins

Karin Bornfeldt

Paul Lampe

Date: 7/27/11

In presenting this disseration in partial fulfillment of the requirements for the doctoral degree at the University of Washington, I agree that the Library shall make its copies freely available for inspection. I further agree that extensive copying of the dissertation is allowable only for scholarly purposes, consistent with "fair use" as prescribed in the U.S. Copyright Law. Requests for copying or reproduction of this dissertation may be referred to ProQuest Information and learning, 300 North Zeeb Road, Ann Arbor, MI 48106-1346, 1-800-521-0600, to whom the author has granted " the right to reproduce and sell (a) copies of the manuscript in microform and/or (b) printed copies of the manuscript made from microform."

Signature _____

Date _____

University of Washington

ABSTRACT

The role of *C. elegans* NHR-49 in regulating global lipid homeostasis

Pranali Pathare

Chair of the Supervisory Committee:
Member, Susan Biggins
Division of Basic Sciences, FHCRC

Mammalian nuclear receptors broadly influence metabolic fitness and serve as popular targets for developing drugs to treat cardiovascular disease, obesity and diabetes. However, the molecular mechanisms and regulatory pathways that govern lipid metabolism, one of the primary energy sources in physiological settings, remain poorly understood. I chose the model organism *C. elegans* to elucidate how nuclear receptors and their regulatory partners maintain global metabolic homeostasis and coordinate multiple signals from different tissues under different contexts to modulate the appropriate transcriptional programs. I set out to explore the impact of the *C. elegans* lipid sensing nuclear receptor NHR-49 on global animal metabolism and physiology. Genome-wide gene expression studies revealed that NHR-49 broadly regulates target genes that fall into several physiological categories including energy balance, lipid binding, lipid degradation, sphingolipid breakdown, lipid remodeling, yolk synthesis/transfer and mitochondrial biogenesis. Worms lacking *nhr-49* function display a host of phenotypes that very closely mirror its gene expression profile. I identified NHR-49 co-factors that influence NHR-49 gene regulation and demonstrated that each receptor accounts for a specific subset of NHR-49 targets. Furthermore, I used deletion mutants of these individual co-factors to delineate their specific contribution to distinct phenotypes of *nhr-49-/-* animals. This work has identified genes and pathways that were

previously not known to be regulated by NHR-49. In addition, ultrastructural analysis revealed that NHR-49 and its partner proteins participate in the orchestration of the influx and efflux of global energy stores into and from different tissues. And, finally, I discovered a previously uncharacterized role for NHR-49 in influencing mitochondrial physiology. Taken together, my findings in *C. elegans* not only provide novel insights into how nuclear receptor transcriptional networks coordinate to regulate global energy metabolism but also reveal the breadth of their influence on different aspects of animal physiology.

TABLE OF CONTENTS

Chapter 3: Role of NHR-49 in regulating the global "lipid economy"

Chapter 4: Role of *C.elegans* NHR-49 in mitochondrial physiology

LIST OF ABBREVIATIONS

Nuclear Receptor (NR)

Nuclear Hormone Receptors (NHR)

Hepatocyte Nuclear Factor Alpha (HNF4-α)

Peroxisome Proliferator Activated Receptor (PPAR)

Quantitative Reverse Transcription Polymerase Chain Reaction (qRT-PCR)

High Pressure Transmission Electron Microscopy (HP-TEM)

Wild-type (WT)

Gas Chromatography/ Mass Spectrometry (GC/MS)

LIST OF FIGURES

LIST OF TABLES

Table Number Page

ACKNOWLEDGEMENTS

I would like to thank Dr. Marc Van Gilst for providing scientific input, feedback and training throughout my graduate career and giving me the opportunity to work on this project. I would also like to extend a special thank you to Dr. Susan Biggins for invaluable support, guidance and mentorship and for being an amazing role model. Thank you also to the rest of the Van Gilst lab past and present for their support and technical guidance. Thank you also to my committee members, Karin Bornfeldt, Jim Priess, Paul Lampe and Michael Rosenfeldt, for scientific feedback and discussion.

Thank you to Prerana Ranjitkar whose constant support and absolute friendship made graduate school a wonderful experience. I also want to acknowledge and thank my family, with out whose love and support this would not be possible. I am so grateful and blessed for the encouragement and blessings of my parents, parents-in-law and sister through the years. I especially want to thank my beloved husband, Navi Mangat for his abundant patience, unquestioning support and unwavering love.

DEDICATION

I dedicate this thesis to my parents, Mr. Prasad and Dr. Prajnya Pathare who always encouraged me to be curious, ask questions and follow my own path. Thank you for your unconditional love and endless support and for always inspiring me to do my best.

CHAPTER 1
INTRODUCTION: NUCLEAR RECEPTOR REGULATION OF LIPID METABOLISM

Lipid metabolism is central to energy homeostasis. Typically fat is broken down and can undergo several potential fates. Fatty acids from the diet can be broken down to generate energy via mitochondrial fatty acid β-oxidation. In addition to providing sufficient levels of ATP, fatty acids are essential components of cellular membranes (phospholipids), long-term energy storage reserves (triglycerides) and even function in signaling pathways (glycolipids) (figure 1.1) (Wymann and Schneiter 2008). Misregulation of any of these processes can lead to inappropriate levels of fatty acids leading to a range of metabolic diseases including obesity, diabetes and cardiovascular disease. The regulatory mechanisms that mediate this very important balance are a class of molecules called nuclear receptors. In this work, we use the model system, *C. elegans* to expand our understanding of how nuclear receptor networks regulate metabolic pathways to modulate lipid homeostasis and influence animal physiology.

Role of Mammalian Nuclear receptors in physiology

Nuclear receptors are ligand-regulated transcription factors designed to sense environmental signals and respond by coordinating diverse physiological programs. They are regulated by small lipophilic ligands that include dietary signals and metabolic intermediates. Upon ligand binding, nuclear receptors undergo a conformational change that switches the regulatory status of the receptor, reprogramming gene expression in target tissues. Nuclear receptors thus exert their effects by directing global changes in gene expression that act to maintain metabolic homeostasis by governing the transcription of genes involved in lipid metabolism, storage, transport, and elimination (Chawla, Repa et al. 2001).

Mammalian lipid sensing nuclear receptors play critical roles in metabolic health by regulating the homeostasis of dietary and endogenous fats, sterols and sugars. The PPAR nuclear receptors are global modulators of fat management controlling fat storage, expenditure, distribution and transport (Desvergne and Wahli 1999). Other lipid sensing nuclear receptors include LXR which governs cholesterol metabolism, transport and storage, and FXR which facilitates transport, metabolism and detoxification of bile acids and phospholipids (Peet, Janowski et al. 1998; Parks, Blanchard et al. 1999) . Finally, HNF-4α is important for lipid and glucose homeostasis (Stoffel and Duncan 1997).

Tremendous progress has been made over the last several years to elucidate the role of nuclear receptors in animal biology. Due to their important roles in regulating fat storage and expenditure in protecting against lipid induced toxicity, lipid sensing nuclear receptors are aggressively targeted for the treatment of conditions associated with the metabolic syndrome, including diabetes, atherosclerosis and obesity. Their important physiological functions and potential as pharmacologic targets makes lipid sensing nuclear receptors an important avenue for disease intervention. In fact, agonists and antagonists for mammalian lipid sensing nuclear receptors have been shown to have significant health benefits for the treatment of metabolic disease. Current research is aimed at defining roles for these receptors in normal development and metabolism as well as better understanding how nuclear receptor dysfunction contributes to diabetes, cancer, cardiovascular disease, obesity, and neuronal disorders (Sonoda, Pei et al. 2008).

C. elegans as a model to understand nuclear receptor biology

Although studies in mammalian systems have provided insights into the molecular mechanisms by which nuclear receptors regulate transcription of target genes, open questions that still remain include the physiological purpose and effects of the extensive set of target genes, as well as the sub-specific impacts of co-factors. Their widespread effect on gene expression and physiology makes it imperative to comprehensively understand nuclear receptor mechanisms in order to develop targeted therapies with minimal side effects. The nematode *C. elegans* is a great model system to

address these shortcomings and is a simple but powerful tool to help characterize the fat regulatory networks and their physiological effects *in vivo*. These microscopic worms are fast growing and easy to maintain. Their total development time from egg to adult takes about three days. Since their genome has been sequenced, it has been shown that many important biological processes like lipid metabolism and fat regulatory pathways are conserved between worms and mammals (Porte, Baskin et al. 2005). In addition, the *C. elegans* knockout consortium makes genetic manipulability and making transgenic animals relatively fast and easy (Consortium 1998).

Discovery of *C. elegans* NHR-49 as a regulator of lipid metabolism

During the evolution of nematodes, the HNF4 family underwent a significant expansion resulting in 284 family members in *C. elegans*, compared to 48 in humans and 21 in flies. Fifteen nuclear receptors have clear homologs in other species, and include relatives of the mammalian HNF4, Vitamin D receptor, COUP-TF, SF1, ROR, PNR, GCNF, TLX as well as the *Drosophila* DHR3, DHR38, E75, E78, DHR78, and DHR96. The other 269 nuclear receptors arose from an ancestral HNF4 (Robinson-Rechavi et al., 2005). We found that one of these nuclear receptors, NHR-49 is an important regulator of fatty acid metabolism. The regulatory targets and physiological effects of NHR-49 are strikingly similar to those of the mammalian lipid sensing nuclear receptors, HNF4-α and PPARα. Even though NHR-49 has a strong sequence similarity to the mammalian HNF4-α, the overall biological effects of *nhr-49* on metabolism, fat storage, and life span are remarkably similar to those of the mammalian PPARs (Van Gilst, Hadjivassiliou et al. 2005). Perhaps most striking is the finding that *nhr-49* and the PPARs, particularly PPARα and PPARδ, positively influence similar genes in multiple metabolic processes, including fatty acid β-oxidation, fatty acid desaturation, and fatty acid binding/transport (Desvergne and Wahli 1999) (Wang, Lee et al. 2003). Moreover, knockout of PPARα or PPARδ can lead to high-fat phenotypes (Wang, Lee et al. 2003) (Costet P, 2008) that are similar to those observed in *nhr-49-/-* animals demonstrating the common physiological effects of these receptors on fat storage. These findings suggest that studying the *C.*

elegans NHR-49 will provide insights into how and why nuclear receptors modulate fat expenditure, fat composition and fat distribution.

Description of Dissertation

The overarching goal of my project was to better understand how nuclear receptors coordinate signals from diverse sources and locations under different environmental conditions to modulate the relevant set of target genes and pathways needed to maintain lipid homeostasis. All organisms must balance energy input and output in order to live. We predicted that disruption of overall nuclear receptor activity via deletions of ligand binding or co-factor interactions would not only disrupt lipid homeostasis but would also reveal specific groups of target genes and associated phenotypes.

The second chapter describes a complete characterization of NHR-49's transcriptional regulatory network. Gene expression data not only confirmed the previously known target genes, but also revealed additional target genes including sphingolipid breakdown and lipid remodeling genes. We also identified three other nuclear receptors NHR-66, NHR-80 and NHR-13 that partner with NHR-49 to regulate distinct subsets of its target genes and as a result contribute to specific aspects of NHR-49 phenotypes. In characterizing NHR-49's transcriptional network, we showed that the control of distinct NHR-49 regulatory modules is based on NHR-49's association with distinct interacting partners. These findings regarding NHR-49's binding partners and their physiological activities also provided considerable insights into the mammalian lipid sensing nuclear receptors, HNF-4α and PPARα. Despite species diversification, nuclear receptors act similarly across taxa to play fundamental roles in detecting intrinsic and environmental signals, and subsequently in coordinating transcriptional cascades that direct reproduction, development, metabolism, and homeostasis (Magner and Antebi 2008). In addition to understanding the transcriptional network and target genes that underlie the physiology controlled by NHR-49, this work revealed several common themes and divergent functions in the context of NHR-49's evolutionarily conserved mammalian homologs.

Chapter three describes the role of NHR-49 and its partner proteins in regulating energy stores and the resultant impact on reproduction. In particular, we used electron microscopy to show that NHR-49 and its partners contribute to the movement of lipid and distribution of glycogen between different organs of the worm and this co-ordination has effects on downstream outputs, like reproduction. One of the limitations in the mammalian receptor field is the missing link between transcriptional studies and physiological models. This work bridges that gap and shows for the first time that the role of nuclear receptors extends well beyond the transcriptional activation and repression of genes, and that they are in fact important mediators of energy transfer and delivery within cells. One of the implications of this work is that nuclear receptors can potentially act as sensors of supply and demand of energy and are in fact capable of modulating the output based on the energy input.

In the fourth chapter, we describe a previously uncharacterized role for NHR-49 in the regulation of mitochondrial physiology. Ultrastructural analysis revealed that animals lacking *nhr-49* function have abnormal mitochondrial morphology. We used deletion mutants of NHR-49 co-factors to show that NHR-49 mediated control of mitochondrial shape and number could be attributed to impaired expression of genes in the fatty acid desaturase and sphingolipid breakdown pathways. This work demonstrates the involvement of very specific genes in the nuclear receptor mediated control of mitochondrial shape and number, paving the way for a better understanding of the transcriptional regulation of mitochondrial biogenesis.

Taken together, our work studying the *C. elegans* NHR-49 contributes new knowledge to the field by providing novel insights into how nuclear receptor transcriptional networks coordinate with each other to regulate global energy metabolism, as well as uncovering the range of nuclear receptor influence on various aspects of animal physiology.

Fig. 1.1

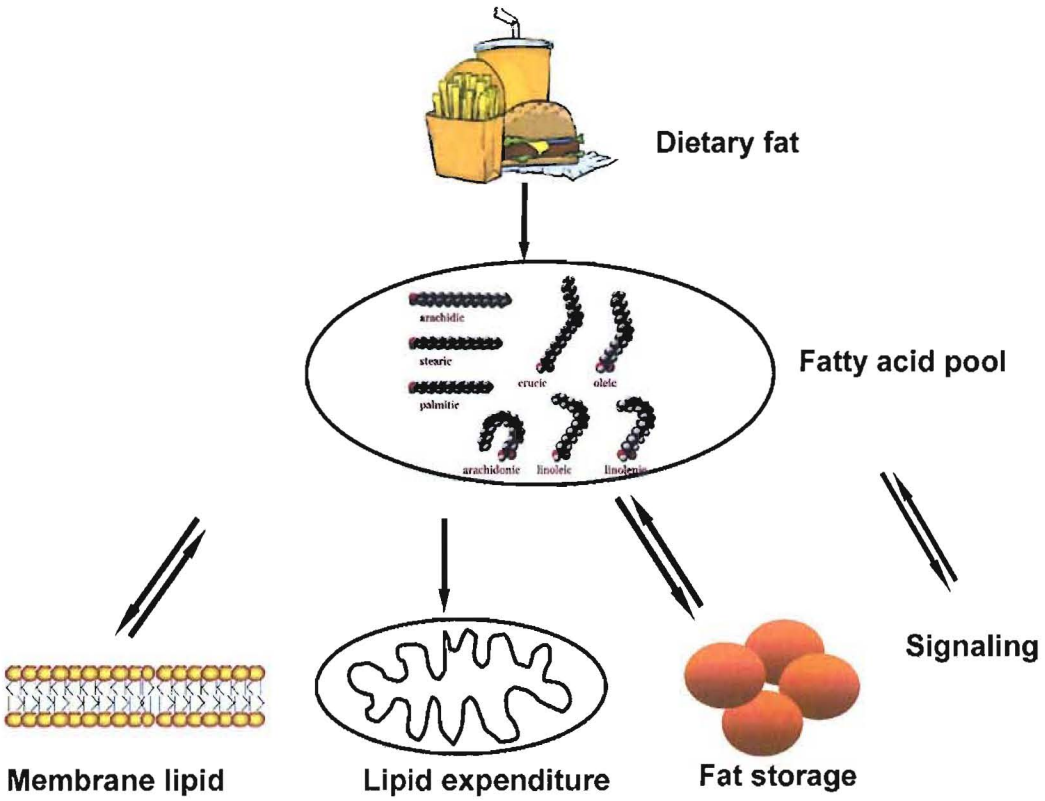

Fig. 1.1 Improper lipid homeostasis is associated with metabolic diseases. Imbalances in any of these processes have been shown to result in a host of diseases.

CHAPTER 2

COORDINATE REGULATION OF LIPID METABOLISM BY A NOVEL NUCLEAR RECEPTOR PARTNERSHIP

Abstract

Global gene expression profiling confirmed that the *C. elegans* lipid sensing nuclear receptor NHR-49 coordinately influences several genes in multiple fat metabolism pathways, through both activation and repression. In addition to confirming that NHR-49 is important in modulating pathways that control fat expenditure and fatty acid saturation, the analysis also revealed that NHR-49 is essential for repressing the expression of genes predicted to participate in sphingolipid processing and lipid remodeling. Here we report the identification and validation of the different NHR-49 co-factors that interact with NHR-49 to selectively modulate distinct aspects of lipid metabolism. Notably, we found that knockout of *nhr-66* specifically abrogated NHR-49 repression of sphingolipid and lipid remodeling targets. In contrast, deletion of *nhr-66* did not impact NHR-49's activation of beta-oxidation and desaturase genes. Our findings thus support a model whereby NHR-49 collaborates with NHR-66 to regulate a system of genes involved in modulating the glycosphingolipid and phospholipid composition. In addition, we found that knockout of *nhr-80* and *nhr-13* affected the expression of NHR-49 regulated fatty acid destaurase genes, but had no impact on any of its other gene targets. Thus, NHR-49 partners with NHR-80 and NHR-13 to regulate the ratio of saturated and unsaturated fat in lipid membranes. Therefore, in characterizing NHR-49's transcriptional network, we found that the control of distinct NHR-49 regulatory modules is based on NHR-49's association with distinct interacting partners. Using deletion mutants, we then parsed out the influence of each of the different lipid pathways on worm physiology. Consistent with NHR-66's repression of NHR-49 regulated sphingolipid metabolism genes, biochemical analysis revealed a significantly altered sphingolipid profile in both *nhr-49-/-* and *nhr-66-/-* animals. Whereas, NHR-80 and NHR-13's modulation of NHR-49 regulated fatty acid desaturase genes contributed towards the shortened lifespan phenotype of *nhr-49-/-* animals. Our findings regarding NHR-49's

binding partners and their physiological activities provide considerable insights into the mammalian lipid sensing nuclear receptors, HNF-4α and PPARα.

Introduction

As a result of our modern day lifestyle and diet, we face a significant threat from a host of chronic diseases including obesity, diabetes and atherosclerosis. These metabolic disorders have been consistently linked to the imbalance between energy consumption and output. Proper energy homeostasis is thus critical. Growing evidence suggests that faulty regulation of fat metabolism promotes metabolic diseases. The control of fat metabolism is often mediated by nuclear receptors. Nuclear receptors are ligand regulated transcription factors that play a central role in the cell's ability to sense, transduce and respond to lipophilic signals by modulating the appropriate target genes (Chawla, Repa et al. 2001) (Evans, Barish et al. 2004).

Nuclear receptors typically exhibit highly conserved modular domains including the zinc-finger DNA binding domain (DBD) and a ligand binding domain (LBD). On binding to a ligand, nuclear receptors mediate transcription through their ability to recognize specific sequences within promoter/enhancer regions of their target genes. Ligand binding affects their activity by inducing structural changes within the LBD, which then alters the receptor's affinity to different co-factor proteins that comprise of co-regulators and binding partner(s). Co-regulators include both co-activators and co-repressors, and are critical in mediating transcriptional responses. Alteration in receptor affinity can thus lead to a change in the transcriptional response i.e., it can result in replacing co-repressors with co-activators to promote transcription of target genes, or in recruiting other nuclear receptors to form homo- or heterodimers to activate or repress a specific set of target genes (Glass and Rosenfeld 2000). Thus binding of distinct co-factors eventually determines how nuclear receptors influence different gene networks.

The Hepatocyte Nuclear Factor 4- alpha (HNF-4α), an example of one such lipid sensing nuclear receptor in mammals, is mainly expressed in liver, pancreas, kidneys and small intestine (Miquerol, Lopez et al. 1994). It orchestrates the regulation of a diverse range of target genes and is especially important in the control of genes involved in glucose and fatty acid homeostasis (Stoffel and Duncan 1997). Consistent with its role in

metabolism, mutations in HNF-4α are associated with both maturity onset diabetes of the young (MODY) and type II diabetes (Yamagata, Furuta et al. 1996). It is not clear how HNF4 protects against diabetes; but it has been reported that mutations in HNF-4α can lead to early death of pancreatic beta-cells resulting in dysfunction and a subsequent decrease in insulin production (Rhodes 2005; Gupta, Gao et al. 2007). In addition, knock-out of HNF-4α in adult mice livers leads to increased hepatocyte accumulation of lipid and also misregulation of several genes involved in glucose and lipid metabolism (Hayhurst, Lee et al. 2001).

Recent data on the HNF4 receptors suggest that this nuclear receptor is highly conserved across species. Mammals have two paralogs of this receptor, HNF4α and HNF4γ. In *C. elegans*, however, the HNF4 family underwent a massive expansion during evolution resulting in 269 HNF4-like receptors (Sluder and Maina 2001; Bertrand, Brunet et al. 2004). Of these 269 family members, only one HNF4-like receptor NHR-49 shares not only a significant structural homology but also displays similar gene expression patterns as the mammalian HNF-4α. These nuclear receptors share a conserved ligand binding pocket, co-activator interface and DNA recognition sequences. They target similar metabolic pathways, like fatty acid β-oxidation, lipid transport and gluconeogenesis, and also respond to a similar physiological cue, like fasting (Dhe-Paganon, Duda et al. 2002; Van Gilst, Hadjivassiliou et al. 2005). Thus, NHR-49 is the worm homolog of mammalian HNF-4α. Also, consistent with mouse liver-specific HNF-4α knockout mutants, *nhr-49-/-* mutants accumulate increased body fat. These animals also undergo premature death reminiscent of the early death observed in HNF-4α – deletion-induced pancreatic beta-cells (Van Gilst, Hadjivassiliou et al. 2005).

An outstanding question that remains is the significance of having so many *C. elegans* HNF4-like receptors. One possibility is that gene expansion could have allowed for worms to distribute the different HNF4-regulated functions and "outsource" them to several individual nuclear receptors. Another possibility is that they simply evolved additional novel functions. In this study, we set out to distinguish between these possibilities by elucidating the NHR-49 regulated gene network and characterizing its

target genes. We also sought to understand the impact of this transcriptional regulation on worm physiology. We have identified NHR-49 co-factors and uncovered additional roles for NHR-49 in the regulation of lipid metabolism. Our findings support a model whereby NHR-49 heterodimerizes with other nuclear receptors and co-regulators to mediate the activation or repression of genes involved in distinct aspects of lipid metabolism. Using knockout strains, we were also able to selectively modulate the effects of individual NHR-49 co-factors to further investigate the shortened lifespan phenotype of *nhr-49-/-* animals.

Results

Full-genome microarray analysis of NHR-49

Initial studies in our lab revealed that NHR-49 promoted two distinct aspects of lipid metabolism, namely fatty acid desaturation and fatty acid beta-oxidation. However, the complete list of NHR-49's regulatory targets was still not known. To address this, we performed transcriptional profiling of NHR-49 to identify all the genes that it regulated. We used full-genome *C. elegans* oligonucleotide microarrays to compare a *nhr-49* (nr2041) deletion strain with N2 wildtype worms. We thus identified a total of 140 genes as regulated more than 2-fold in the *nhr-49* deletion strain. The Wormbase annotation and fold change of the top activated and repressed genes are listed in table 2.1and 2.2. The strongest activated genes include the previously known targets of NHR-49 namely the fatty acid beta-oxidation and fatty acid desaturase genes. Of the strongest repressed genes, these experiments uncovered new NHR-49 targets that include genes involved in sphingolipid breakdown, lipid remodeling and xenobiotic detoxification.

Identification of additional factors that participate in regulation of NHR-49 target genes

Nuclear receptors never act alone and often interact with other nuclear receptors to form heterodimers, or act with other co-factors to promote or inhibit gene expression.

We hypothesized that NHR-49 differentially regulates its distinct target genes by interacting with specific transcriptional co-factors. Yeast-two hybrid experiments (performed in theYamamoto lab) that used NHR-49 LBD as the bait protein identified numerous proteins that directly bind to NHR-49 (table 2.3), including numerous other nuclear receptors. We then systematically evaluated each of these by using their deletion mutants and performing qRT-PCR to investigate if they affected NHR-49 gene regulation. The qRT-PCR panel included the topmost NHR-49 activated and repressed genes (see primer pairs, table 2.4 and 2.5). In doing this, we found 2 potential co-factors that controlled different NHR-49 target genes: NHR-66 and NHR-13. In addition to these three candidates, NHR-80 had previously been shown to regulate the fatty acid desaturase genes (Watts and Browse 2002). Since these genes overlapped with NHR-49's gene targets, we chose to include NHR-80 in our analysis.

NHR-49 physically interacts with NHR-66, NHR-80 and NHR-13

We next wanted to assess if NHR-49 directly binds to these candidate interacting nuclear receptors. We performed *in vitro* GST pull-down assays to verify NHR-49's interaction with full length NHR-66, NHR-80 and NHR-13 proteins. Since earlier work (yeast-two-hybrid) had shown that NHR-49 was capable of interacting with itself and therefore forming homodimers, we used NHR-49 as a positive control. We performed pull-down assays with *in vitro* translated ^{35}S-methionine labeled NHR-49, NHR-66, NHR-80 and NHR-13 and purified glutathione-S-transferase (GST)-tagged NHR-49. GST-NHR-49 successfully formed a homodimer by pulling radiolabeled NHR-49 down and was also able to form heterodimers with NHR-66, NHR-80 and NHR-13. In other words, binding reactions consistently demonstrated the interaction of labeled NHR-49, NHR-66, NHR-80 and NHR-13 with GST-NHR-49 but not with the GST alone control (figure 2.1).

NHR-66 represses NHR-49-regulated sphingolipid and lipid remodeling genes

Once we established that NHR-49 directly binds to NHR-66, NHR-80 and NHR-13, we next wanted to characterize their common NHR-49 dependent target genes. The deletion of *nhr-66* (ok940) resulted in the upregulation of most of NHR-49's repressed genes. We found that NHR-66 is required for the repression of 27 out of 30 of NHR-49's repressed genes. In both *nhr-49* and *nhr-66* mutants, the expression of sphingolipid and lipid remodeling genes are strongly induced. These genes include the sphingolipid breakdown enzymes like acid ceramidase, glycosyl hydrolase, sphingosine-phosphate lyase and lipid remodeling genes like phospholipases, TAG lipases and O-acyltransferases. In contrast, *nhr-66* mutants did not show any change in the expression profile of *nhr-49* activated genes, like those involved in beta-oxidation and desaturation (figures 2.2A and 2.2B). These results strongly imply that NHR-49 acts with NHR-66 to repress the transcription of sphingolipid and lipid remodeling genes.

To address if NHR-66 was regulating only NHR-49 dependent genes or if NHR-66 regulated additional genes of its own, we performed a microarray analysis on *nhr-66-/-* mutants. The list of the strongest NHR-66 upregulated and downregulated genes is presented in table 2.6 and 2.7, respectively. Thus our analyses suggested that NHR-66 is not only a transcriptional partner required for NHR-49 gene repression, but may also be part of other transcriptional networks regulating additional genes independent of those controlled by NHR-49.

NHR-80 and NHR-13 activates NHR-49-regulated fatty acid desaturase genes

On the other hand, we found that the *nhr-80* (tm1011) and *nhr-13* (VC 1656) deletion mutants exhibit a decrease in expression of fatty acid desaturase genes. In other words, NHR-80 and NHR-13 are important for the activation of NHR-49 regulated fatty acid desaturase genes: *fat-7*, *fat-5* and *fat-6*. These are members of the Δ9 fatty acid desaturases and are key enzymes in fatty acid metabolism. Their function is to introduce a double bond in saturated fatty acid chains to generate monounsaturated fatty acids (MUFAs). Production of MUFAs by these desaturases is the first step of the desaturation pathway and these MUFAs are incorporated into lipids such as phospholipids and

triglycerides where they play essential roles in membrane fluidity and energy storage (Ntambi 1995). The *nhr-80-/-* and *nhr-13-/-* animals had no impact on NHR-49's beta-oxidation genes or its sphingolipid metabolism and remodeling genes (figures 2.2A and 2.2B). These results suggest that NHR-49 associates with NHR-80 and NHR-13 to regulate the ratio of saturated and unsaturated fat in lipid membranes. Again, our NHR-80 data is in accordance with what was previously shown by the Watts lab (Watts and Browse 2002).

We also performed a full genome-wide microarray analysis on *nhr-80-/-* to determine if NHR-80 had regulatory targets independent of NHR-49. The list of the strongest NHR-80 upregulated and downregulated genes is presented in table 2.8 and 2.9, respectively. Thus our analyses showed that in addition to interacting with NHR-49, NHR-80 could potentially act with other binding partners to regulate other sets of genes.

NHR-49's regulation of desaturases is contributing to lifespan

The binding assay and gene expression data together support a model whereby the control of distinct NHR-49 regulatory modules is based on NHR-49's association with distinct interacting partner proteins. In other words, the regulatory targets of NHR-49 are separable based on what binding partner NHR-49 interacts with. Using deletion mutants of each interacting NHR-49 partner, we wanted to determine the individual effects of the different co-factors on the phenotype of *nhr-49-/-* mutants. We chose to investigate the reduced lifespan phenotype of *nhr-49-/-* animals. We performed lifespan assays on *nhr-66-/-* mutants to examine the effect of NHR-49's repressed genes on lifespan. These mutants had no effect on lifespan, and we thus ruled out the possibility that the NHR-49-regulated sphingolipid and lipid remodeling genes played a role in the reduced lifespan phenotype. Next, we performed lifespan assays on *nhr-80-/-* and *nhr-13-/-* mutants. At 20 ^{0}C, these mutants were significantly shorter-lived with a lifespan of 13.19+/-0.38 days and 14.17+/-0.4 days respectively, compared to that of 17.35+/-0.34 days observed in wildtype worms. In fact, the *nhr-80-/-; nhr-13-/-* double mutant had a lifespan of 12 days comparable to that of the *nhr-49-/-* mutant that has a lifespan of 9.52+/-0.23 days. These

results suggest that the reduced expression of fatty acid desaturases observed in the *nhr-80-/-* and *nhr-13-/-* mutants might be contributing to the shortened lifespan of *nhr-49-/-* animals (figures 2.3A and 2.3B and table 2.11).

These observations are in accordance with previous published work demonstrating that shortened lifespan phenotype results from lowered expression of the *fat-7* SCD (Van Gilst, Hadjivassiliou et al. 2005). In addition, both *nhr-49-/-* and worms grown on *fat-7* RNAi have a concomitant increase in the levels of saturated fat. More specifically, the reduction in desaturase levels results in the alteration of the ratio between stearic acid and oleic acid (C18:0/C18:1n9) to almost 4 times higher (about 3.74+/-0.33 in *nhr-49-/-* animals) than that seen in wildtype animals. We thus evaluated the saturated fat levels of the deletion mutants. We used GC-mass spec to measure the abundance of individual lipid species and then compared the ratio of C18:0 to C18:1 to that of *nhr-49-/-* mutants. We found that like the *nhr-49-/-* mutants, the *nhr-80-/-;nhr-13-/-* double mutants also had higher value of C18:0/C18:1n9 (2.99+/-0.22) relative to wildtype (0.98+/-0.06) (figure 2.4A and table 2.12). In fact, we see a strong inverse correlation (r^2=0.86) between the level of saturated fat and the duration of mean worm lifespan (figure 2.4b). This observation supports the notion that the accumulation of excess saturated fat as a result of reduced fatty acid desaturase expression is playing a role in the early death phenotype of the *nhr-49-/-* mutant. These results also suggest that NHR-49's interaction with NHR-80 and NHR-13 is contributing to the shortened lifespan phenotype that is observed in *nhr-49-/-* mutants.

nhr-49-/- and *nhr-66-/-* animals have an altered sphingolipid composition

The gene expression data also predicted that deletion of *nhr-49* and *nhr-66* would lead to the increased breakdown of glycolipids, as well as their metabolic intermediates. To assess the contribution of NHR-66 to the phenotype of *nhr-49-/-* animals, we separated total lipid from N2 (wildtype), *nhr-49-/-* and *nhr-66 -/-* worms into their glycolipid species and fractionated them using thin layer chromatography (TLC). As expected, we found that deletion of *nhr-49* and *nhr-66* both affect the composition of

simple glycolipids. In particular, we see a decreased abundance of lactosyl-ceramide in mutant worms as compared to wildtype N2 worms. In contrast, the ratio of abundance of galactosyl ceramide is increased in mutant worms as compared to N2s. This is consistent with the qRT-PCR data where both *nhr-49-/-* and *nhr-66-/-* mutants were shown to have increased expression of glycosyl hydrolase that breaks down lactosyl ceramide and increased expression of galactosyl ceramide transferase that degrades ceramide into galactosyl ceramide (figure 2.5). This data suggests that NHR-49 collaborates with NHR-66 to regulate a system of genes involved in modulating the glycosphingolipid membrane composition. These observations also confirm that NHR-49's interaction with NHR-66 is contributing to this altered sphingolipid composition phenotype in *nhr-49-/-* mutants.

Discussion

In addition to NHR-49's affects on genes involved in fatty acid beta-oxidation and fatty acid desaturation, our present study has revealed a previously uncharacterized group of NHR-49 targets, namely genes involved in the repression of sphingolipid processing and lipid remodeling. We also identified several NHR-49 interacting partner receptors, NHR-66, NHR-80 and NHR-13 that discern between and modulate only selective NHR-49 dependent pathways. Furthermore, each of these regulatory modules of NHR-49 is separable and contributes to a specific phenotype of the worm. In characterizing NHR-49's transcriptional network and studying the resulting influence on physiology, our findings will better inform us of the common evolutionary history of all HNF-4 receptors across species and their conserved metabolic pathways and physiological functions.

Ongoing dispute over the number and identity of HNF-4α's target genes has yet to be worked out. Several studies have reported varying number of genes regulated by HNF-4α, employing a range of experimental approaches, including transient transfection of HNF-4α into a hepatoma cell line, a rat insulinoma cell line, and a human kidney cell line (Naiki, Nagaki et al. 2002; Lucas, Grigo et al. 2005). Notably, Odom *et al* performed chIP on chip to identify promoters occupied by HNF-4α in the human liver and pancreas

and revealed an extremely high number of HNF-4α –targeted promoters; 1575 potential HNF4 target genes (Odom, Zizlsperger et al. 2004). In contrast, a study by Gupta *et al* analyzing at gene expression regulation in pancreatic cells of an HNF-4α conditional knockout model, identified only 133 genes as HNF-4α regulated (Gupta, Gao et al. 2007). This disparity in the number of HNF-4α target genes is still not resolved. We addressed this issue in our study by using gene expression profiling to comprehensively identify all of the *C. elegans* HNF-4α homolog, NHR-49's target genes. These experiments revealed a novel role for NHR-49 in the regulation of genes involved in membrane lipid metabolism, particularly glycosphingolipid processing. Interestingly, a connection has not yet been reported for the role of HNF-4α in regulating sphingolipid metabolism in genome-wide expression studies in mammals.

In addition to the controversy over the target genes, the different co-factors of mammalian HNF-4α responsible for influencing distinct aspects of gene expression have not been fully identified. Since the core functions of HNF-4 have been conserved from yeast to drosophila to mammals, it is reasonable to expect that HNF-4 co-factors in *C. elegans* would behave in a functionally similar manner to those in mammals. Furthermore, since the co-activator interface that is important in mediating the interaction of co-factors to nuclear receptors is perfectly conserved between HNF-4α and NHR-49, our findings are of particular relevance to mammalian systems. We have thus taken advantage of *C. elegans* genetics to successfully identify NHR-49's multiple partners and confirm their interaction with NHR-49. Notably, we found that knockout of *nhr-66* affected only a subset of NHR-49 targets: sphingolipid and lipid remodeling target genes and knockout of *nhr-80* and *nhr-13* affected the expression of NHR-49-regulated fatty acid desaturases. In addition, *in vitro* binding assays further confirmed that NHR-49 can physically interact with NHR-66, NHR-80 and NHR-13. We thus suggest a model whereby NHR-49 and NHR-66 heterodimerize to regulate a system of genes that mediate the breakdown of glycolipids and remodeling of lipid membranes. And, NHR-49 together with NHR-80 or NHR-13 sense and regulate the balance between saturated and unsaturated fat (figure 2.6).

Besides the three NHR-49 binding partners, the two hybrid assay had also identified the *C. elegans* Mediator subunit, MDT-15. MDT-15 has previously been shown to act as a transcriptional co-activator of NHR-49 necessary in the regulation of NHR-49's activated genes including the fatty acid beta-oxidation and desaturase genes (Taubert, Van Gilst et al. 2006). Even though co-activators typically promote gene expression, their activities can be somewhat nuanced. For instance, under certain promoter contexts, co-activators can repress gene expression in a gene-specific manner. We found that MDT-15 indeed regulated a subset of NHR-49's repressed genes (data not shown). It cannot be ruled out, however that these NHR-49 repressed genes are upregulated as a means of compensating for impaired NHR-49 activated genes, like beta-oxidation or desaturases. However, it is important to note that (1) NHR-66 regulates these genes in the absence of impaired beta-oxidation and desaturation (2) RNAi of beta-oxidation genes and RNAi of *fat-7* did not result in upregulation of NHR-49's repressed genes. Thus MDT-15 can potentially function to repress NHR-49 gene expression in a manner that we do not yet understand.

Another interesting finding of this study is the complexity of the NHR-49 regulatory network. Our microarray data suggests that in addition to the common target genes jointly regulated by NHR-49/NHR-66 and NHR-49/NHR-80, NHR-66 and NHR-80 regulate additional genes independent of that of NHR-49. Essentially, both NHR-66 and NHR-80 have their own network of players distinct from those involved in NHR-49 gene transcription.

In addition, our lifespan analysis revealed that NHR-80 and NHR-13 are the regulatory modules contributing to the early death of *nhr-49-/-* deletion mutants. i.e. NHR-49's interaction with NHR-80 and NHR-13 modulating the levels of saturated and unsaturated fat play a part in the shortened lifespan phenotype of *nhr-49-/-* deletion mutants. Furthermore, there is a significant correlation between the ratio of C18:0 to C18:1n9 and reduced mean lifespan leading us to speculate that NHR-49 maybe protecting against early death by preventing an excessive accumulation of saturated fat. This is especially interesting given that the mechanism of how mammalian HNF-4α

protects against diabetes is still not known. Several studies have used both *in vitro* and animal models to show that pancreatic beta cells are highly susceptible to saturated fat-induced apoptosis or lipotoxicity (Shimabukuro, Higa et al. 1998; Unger and Zhou 2001). Moreover, additional studies provide further evidence that overexpressing SCD protects against this lipotoxicity (Listenberger, Han et al. 2003; Peter, Weigert et al. 2008). These observations raise the possibility that the mammalian HNF-4α might be employing a similar mechanism as the *C. elegans* NHR-49 to protect against premature death. Although this hypothesis needs to be further tested, it seems very reasonable given NHR-49's structural homology to HNF4 and its physiological activities.

Despite NHR-49's strong structural homology to HNF-4α, functionally NHR-49 more closely resembles the mammalian nuclear receptor PPARα. Like NHR-49, PPARα activates fasting-response genes involved in gluconeogenesis and also regulates fatty acid beta-oxidation and lipid transport. Similar observations were made in drosophila where dHNF4 was reported to behave functionally analogous to that of mammalian PPAR-α, regulating beta-oxidation and playing a role in the starvation response (Palanker, Tennessen et al. 2009). Consistent with their role in metabolism and fasting, PPAR-α mutant mice have also been shown to display a defective response to starvation and have enlarged lipid droplets in their liver (Hayhurst, Lee et al. 2001). In fact, even *S .cerevisiae* shares common heterodimeric partners, Oaf1/Pip2 that are strikingly similar in structure and function to PPAR-α and its binding partner RXR (Phelps, Gburcik et al. 2006). Thus, in comparing HNF-4 and HNF-4-like nuclear receptors across species (table 2.13) from yeast to mammals, a common theme that emerges is the conservation of its role in lipid metabolism pathways all throughout evolution. It is tempting to speculate that the ancestral role of HNF-4 was adopted by PPAR-α to primarily include mobilization of stored energy during nutrient deprivation and the regulation of beta-oxidation, while the other functions of HNF-4 were either retained or outsourced to additional nuclear receptors.

By the same reasoning, we speculate that when the HNF-4 gene underwent a massive expansion in *C. elegans*, the precursor HNF-4 receptor allocated its various

functions to different nuclear receptors. Paralogs of the HNF-4 receptor in nematodes could then have been selected for divergent functions that included sphingolipid metabolism and xenobiotic metabolism. In other words, just like PPAR/RXR adopted specific HNF-4 roles in mammals, NHR-49 heterodimerized with different binding partners to adopt individual tasks that encompassed the numerous functions of the precursor nematode HNF-4. This is particularly intriguing given the striking absence of any *C. elegans* orthologs of RXR-like molecules that in mammals/fruit flies/yeast heterodimerize with a range of interacting proteins. It might be possible that sometime in evolution *C. elegans* lost an RXR ortholog but since NHR-49 behaves as a promiscuous partner forming heterodimers with other nuclear receptors, it may have assumed an RXR-like function. i.e., NHR-49 could serve as an ancestral binding partner reminiscent of the mammalian RXR. *C. elegans* thus represents a class of animals that switched from solely using HNF-4 receptors to regulate lipid metabolism to those that began to employ different heterodimeric partners to regulate distinct metabolic pathways.

The role of mammalian HNF-4α however is not limited to energy metabolism; HNF-4α is also involved in several physiological processes such as hepatocyte development and differentiation, blood coagulation and immune function. A possible explanation for this could be that the mammalian HNF-4 receptors evolved novel functions to accommodate these additional roles, as organisms became more complex.

Besides the conservation of common metabolic pathways, HNF-4α also shares conserved co-regulatory modules, across species. For example, the *C. elegans* co-activator MDT-15 and the mammalian co-activator PGC-1α collaborate with NHR-49 and PPAR-α respectively in their response to fasting (Taubert, Van Gilst et al. 2006).

In closing, our study has identified distinct binding partners that modulate specific pathways of NHR-49 activity. Given the conservation of HNF-4 structure, function and regulatory modules across species, it is very plausible that mammalian HNF-4α utilizes similar mechanisms as that of *C. elegans* NHR-49, thus informing us of ways to selectively modulate its activity. Exploring these possibilities can assist in

pharmacological efforts to manipulate mammalian HNF-4α for specific desired outcomes without any detrimental side-effects.

Materials and methods

Nematode strains and growth conditions

C. elegans strains N2-Bristol (wildtype), *nhr-49* (nr2041), *nhr-66* (ok940), *nhr-80* (tm1011) and *nhr-13* (VC1656) were used for all experiments. Worms were maintained by standard techniques at 20°C. Single-worm PCR was used to determine the genotype of worms during crossing to generate *nhr-80-/-; nhr-13-/-* double-mutant lines. For mRNA and GC/MS analysis, worm embryos were allowed to hatch on unseeded nematode growth media (NGM)-lite plates overnight at 20 °C. The next day, synchronized L1 larvae were plated onto NGM-lite plates seeded with Escherichia coli strain OP50. Worms were grown to early L4s at 20°C, harvested, washed three times with M9 and flash-frozen in liquid N_2.

Preparation of total nematode mRNA

C. elegans strains N2-Bristol (wildtype), *nhr-49* (nr2041), *nhr-66* (ok940), *nhr-80* (tm1011) and *nhr-13* (VC1656) were grown at 20°C on high-growth plates seeded with OP50 bacteria. Gravid adults from 10 10-cm plates were bleached, and embryos were dispersed onto 15-cm nematode growth media (NGM)-lite plates seeded with OP50. Worms at L4 stage were harvested, washed twice with M9, and frozen in liquid nitrogen. For RNA preparation, worms were thawed at 65°C for 10 min, and RNA was isolated using the Tri-Reagent Kit (Molecular Research Center, Cincinnati, Ohio, United States). Isolated total RNA was subjected to DNAase treatment and further purification using RNAeasy (Qiagen, Valencia, California).

qRT-PCR and microarray analysis

cDNA was prepared from 5 μg of total RNA in a 100-μl reaction using the Protoscript cDNA preparation kit (New England Biolabs, Beverly, Massachusetts, United States). Primer pairs were diluted into 96-well cell culture plates at a concentration of 3 μM. Next, 30-μl PCR reactions were prepared in 96-well plates. Each PCR reaction was carried out with TaqDNA Polymerase (Invitrogen, Carlsbad, California, United States) and consisted of the following reaction mixture: 0.3 μM primers, 1/500th of the cDNA reaction (corresponds to cDNA derived from 10 ng of total RNA), 125 μM dNTPs, 1.5 mM $MgCl_2$, and 1X reaction buffer (20 mM Tris pH 8.4, 50 mM KCl). 0.15 μl (0.75 units) of TaqDNA Polymerase was used for each reaction. Formation of double-stranded DNA product was monitored using SYBR-Green (Molecular Probes, Eugene, Oregon, United States). Data were collected using RNA from at least three independent C. elegans growths. To determine the relationship between mRNA abundance and PCR cycle number, all primer sets were calibrated using serial dilutions of cDNA preparations. qRT-PCR primers were designed using Primer3 software.

For microarray analysis, RNA was then labeled with Cy3 or Cy5 and hybridized to Washington University manufactured C. elegans microarrays. Data was obtained from three independent biological replicates and analyzed using GenePix Pro 6.0 software. Ratios were calculated using background corrected, and normalized data (global mean). qPCR was performed using a BioRad iCycler (MyiQ Single color).

Fatty acid analysis

Fatty acids were isolated from 10,000 L4 animals grown on a single 15-cm NGM-Lite plate. Total lipids were extracted and converted to fatty acid methyl esters (FAMEs) as described (Watts and Browse). After incubation at 80°C for 1 hour the samples were cooled and the FAMEs were extracted by adding water and hexane. FAMEs were analyzed for fatty acid composition by gas chromatography/mass spectrometry (GC/MS) (Agilent 5975GC, 6920MS). Peaks were assigned using fatty acid standards. For

sphingolipid analysis, the lipids were further separated using a pre-equilibrated column and the different lipid fractions, including the glycolipids were eluted. The samples from the different mutant strains were then run on a TLC plate.

Plasmids

The PCR products of the full length NHR-49, NHR-66, NHR-80 and NHR-13 were inserted into the expression vector pcs-2 that was generously given to us by Dr.B Eisenmann (FHCRC). For bacterial expression, GST-NHR-49 was constructed by inserting BamH1-NHR-49 coding sequence-EcoR1 into PGEX-2T vector. All the clones were confirmed by sequencing analysis.

GST-pull down assays

GST-fused NHR-49 (GST-NHR-49) was expressed in the Escherichia coli BL21 (DE3) strain and purified using glutathione-Sepharose 4B beads. ^{35}S-methionine-labeled proteins were prepared by in vitro translation using the TNT-coupled transcription/ translation system with conditions as described by the manufacturer (Promega: Madison, WI). In vitro protein-protein interaction assays were carried out.

Lifespan assays

Approximately 30–40 L1 worms were transferred to 6-cm plates seeded with L4440 RNAi bacteria and life-span assays were carried out at 20 °C as described previously. The L4 stage was counted as day 0. Adults were transferred to new plates daily until progeny production had ceased. Animals were considered dead when they no longer responded to a gentle tap with a worm pick. Life span curves and statistical data including p-values from Log-rank (Mantel-Cox) test were generated using GraphPad Prism version 5 software (GraphPad Software, San Diego, California, USA).

Fig. 2.1

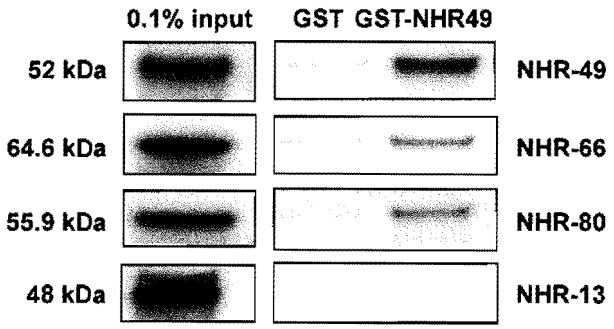

Fig. 2.1. NHR-49 physically interacts with NHR-49, NHR-66, NHR-80 and NHR-13 *in vitro*. Pull-down assays showing in vitro translated ^{35}S-methionine labeled NHR-49, NHR-66, NHR-80 and NHR-13 binding purified GST-NHR-49 fusion protein versus purified GST-alone control. The protein mixtures of ^{35}S-methionine-labeled NHRs were incubated with glutathione-sepharose 4B beads and analyzed by SDS-PAGE (4-12%). The input represents 0.1% of the labeled proteins used for the pull down assays. The experiments were repeated three times.

Fig. 2.2

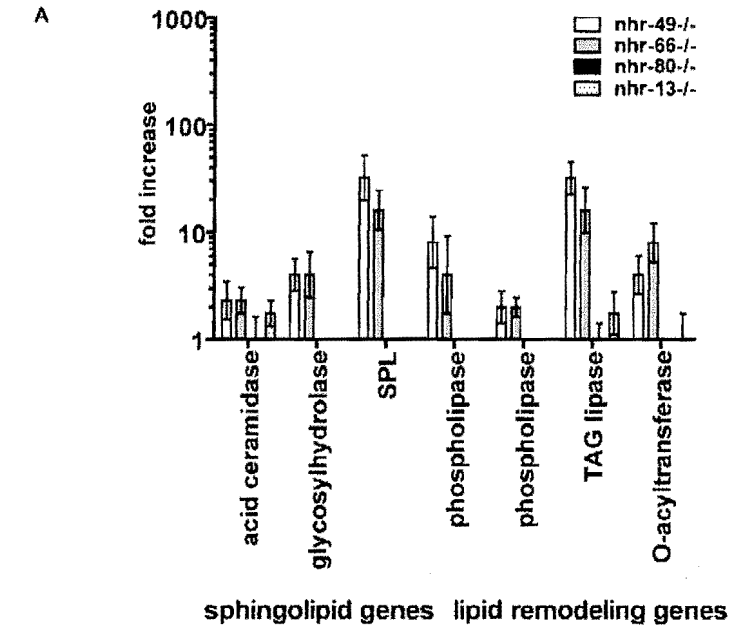
A
1000
100
10
1
fold increase
nhr-49-/-
nhr-66-/-
nhr-80-/-
nhr-13-/-
acid ceramidase
glycosylhydrolase
SPL
phospholipase
phospholipase
TAG lipase
O-acyltransferase
sphingolipid genes
lipid remodeling genes

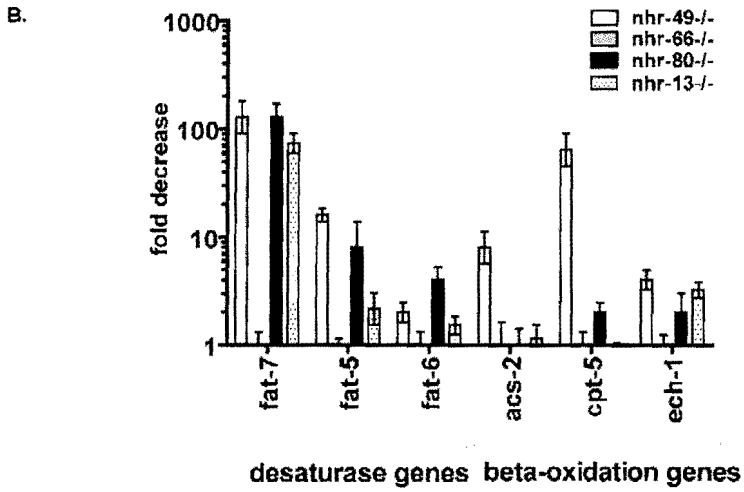
B.
1000
100
10
1
fold decrease
nhr-49-/-
nhr-66-/-
nhr-80-/-
nhr-13-/-
fat-7
fat-5
fat-6
acs-2
cpt-5
ech-1
desaturase genes
beta-oxidation genes

Fig. 2.3

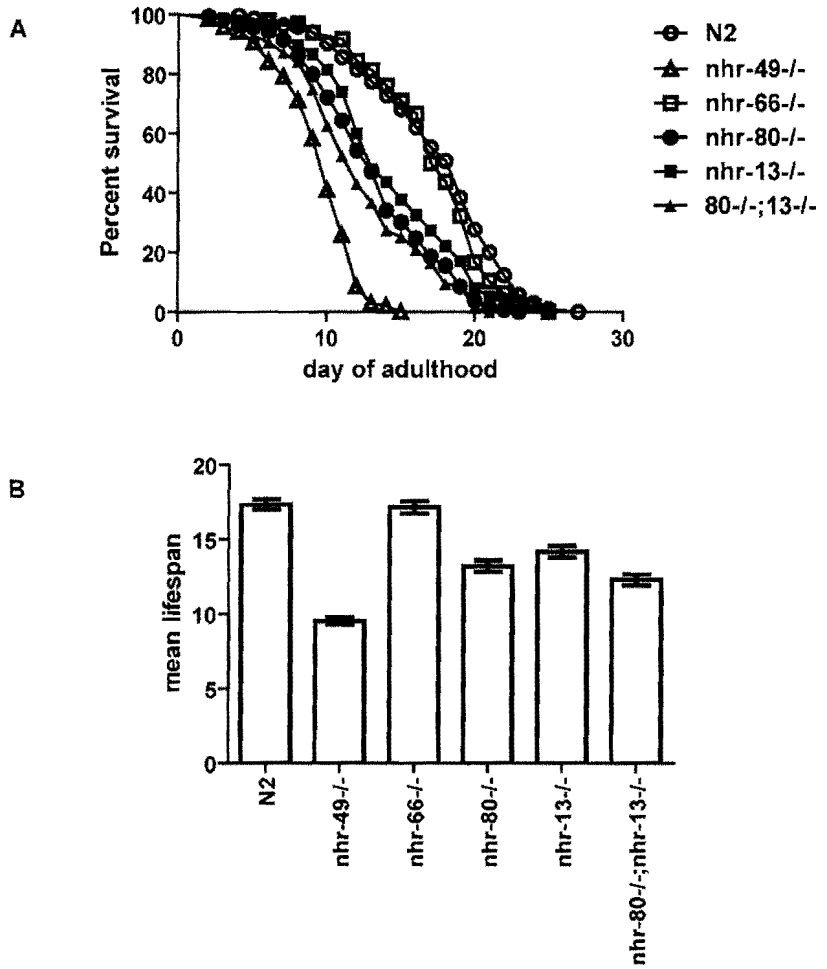

Figure 2.3. Double mutants *nhr-80-/-; nhr-13* have a reduced lifespan similar to that of *nhr-49-/-* animals.
A. The percentage of animals remaining alive is plotted against animal age. Adult lifespan survival curves of WT (empty circles), *nhr-49* (2041) (empty triangles), *nhr-66* (ok940) (empty squares), *nhr-80* (tm1011) (filled circles), *nhr-13* (vc1656) (filled squares) and double mutant *nhr-80-/-; nhr-13-/-*(filled triangles) animals. The curves shown represent pooled data from at least 4 independent experiments.
B. The bar graph represents the combined mean (+/-SEM) adult lifespan from at least 4 independent experiments.

Fig. 2.4

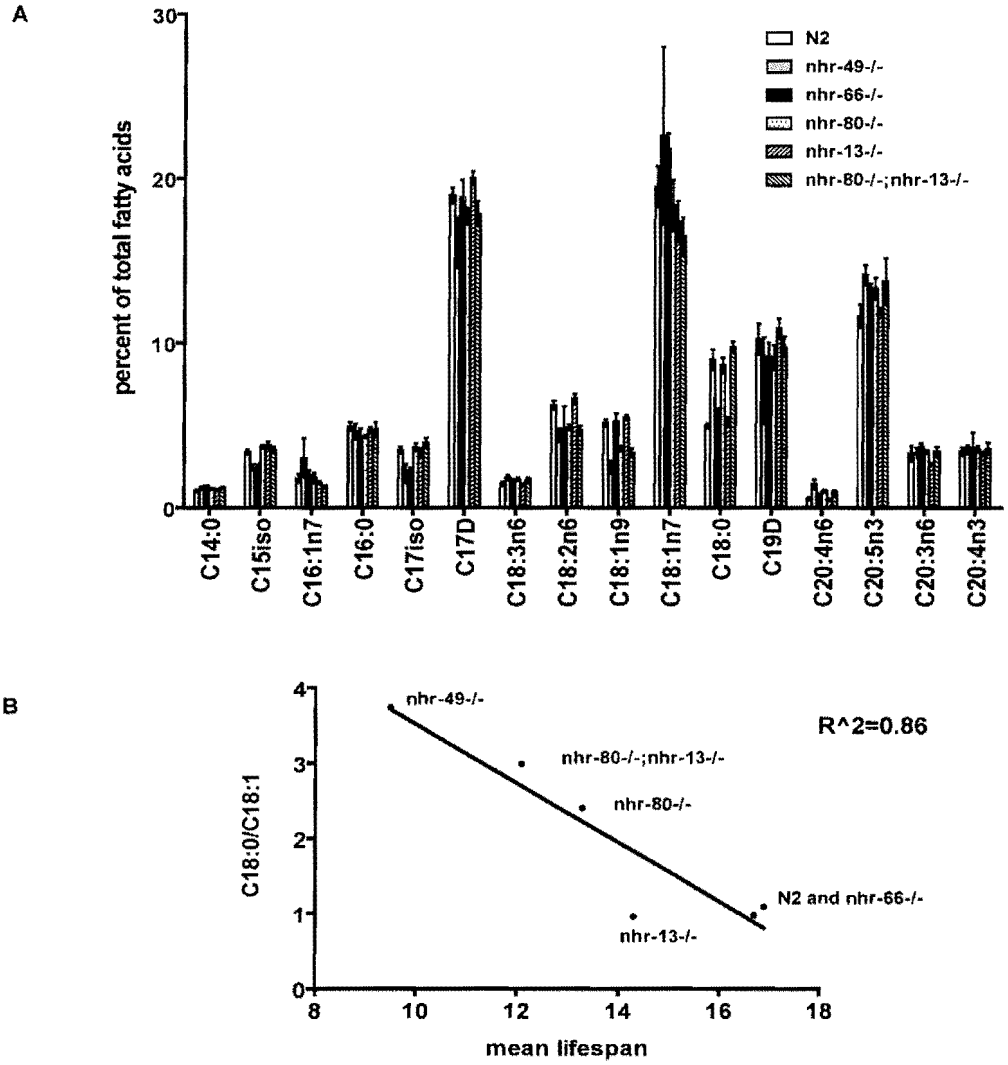

Figure 2.4. Higher levels of saturated fat in *nhr-80-/-;nhr-13-/-* and *nhr-49-/-* animals correlate to shortened lifespans.
A. Relative abundance of individual fatty acid species expressed as percentage of total measured fatty acid. Fatty acids were isolated and quantified by GC/MS from WT (white bars), *nhr-49-/-* (grey bars), *nhr-66-/-* (black bars), *nhr-80-/-* (horizontal stripes), *nhr-13-/-* (vertical stripes) and *nhr-80-/-; nhr-13-/-* (dotted bars) animals. Error bars represent standard error. Data represent the mean of at least 4 independent experiments.
B. Correlation between the ratio of C18:0 to C18:1n9 and mean lifespan.

Fig. 2.5

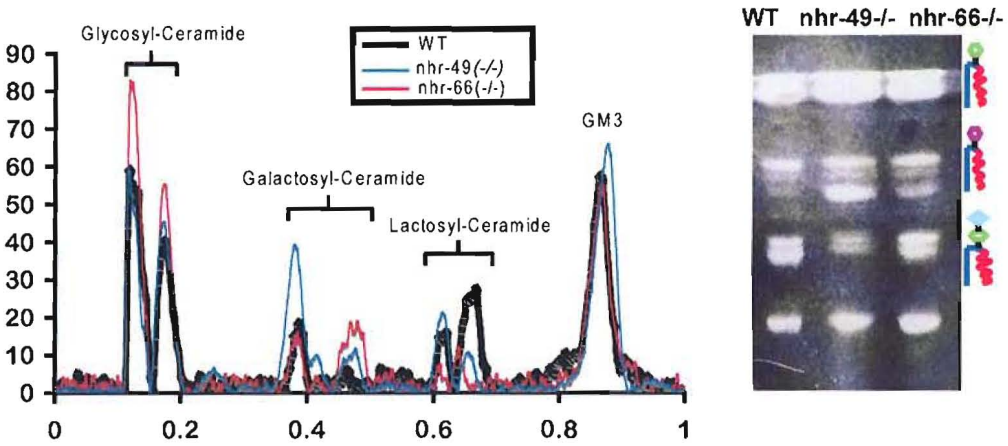

Figure 2.5. Altered sphingolipid profile in *nhr-49-/-* and *nhr-66-/-* animals compared to wildtype controls.
Quantification of different sphingolipid species obtained from wildtype, *nhr-49-/-* and *nhr-66-/-* animals using Thin Layer Chromatography (TLC).

Fig. 2.6

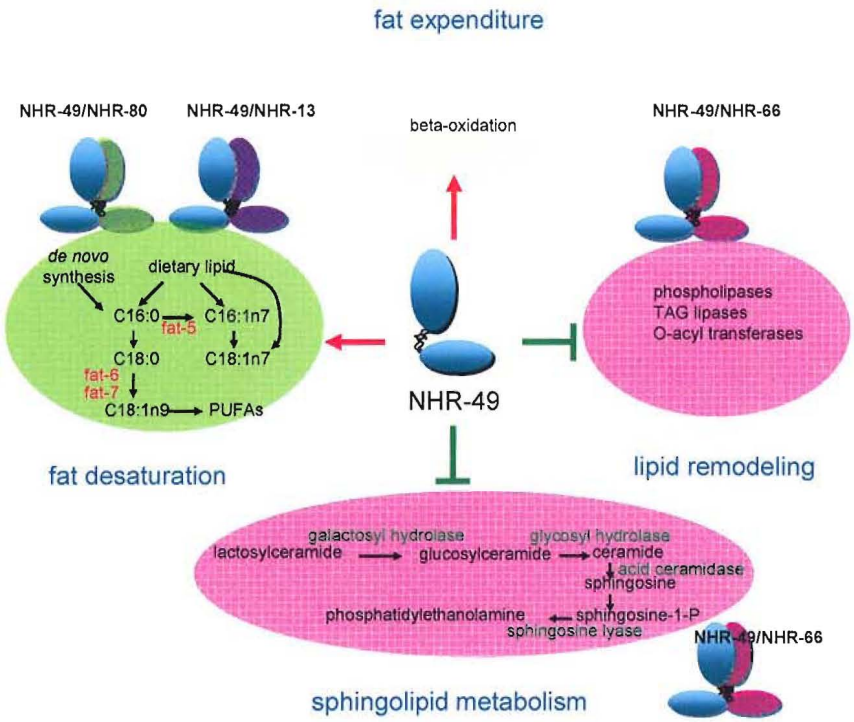

Figure 2.6. Proposed model of NHR-49 transcriptional network. NHR-49 (in blue) interacts with NHR-66 (in pink) and is necessary for the repression of genes involved in sphingolipid processing and lipid remodeling. NHR-49 (in blue) also binds to NHR-80 (in green) and NHR-13 (in purple) to regulate the activation of the desaturase genes.

Table 2.1. List of genes upregulated in *nhr-49-/-* compared to wildtype N2 animals. The data is a result of analysis of three independent mRNA isolations and microarray hybridizations.

Table 2.1

Genepairs name	sequence description	fold change
B0348.2	small integral membrane lysosome	17.8
B0222.4	tag-38, sphingosine phosphate lyase	12.8
F45E4.1	arf-1, ADP ribosylation factor	7.07
R08H2.9	nhr-269	6.8
Y65B4BR.1	phospholipase	4.5
Y37H2A.11	microtubule associated lipoprotein	4.49
C29F3.5	sugar binding lectin	4.39
ZK218.5	secreted surface protein	4.2
W03B1.6	integral membrane O-acyltransferase	4.17
ZK617.2	TAG lipase	4.12
F27E5.1	acid ceramidase	4.11
E02H9.5	glycosyl hydrolase	4.07
T10B9.1	cyp13A4	3.9
C36C5.14		3.9
C29F3.2	sonic hedgehog	3.95
T24C4.4		3.88
F54F3.3	TAG lipase	3.7
ZK218.3	secreted surface protein	3.6
Y46C8AL.4	c-lectin	3.59
C47F8.5	galactosyl transferase	3.43
C47A10.1	pgp-9 abc transporter	3.3
C04G6.5	salt-stress induced peptide	3.23
F35E8.8	gst-38	3.21
C47F8.8	nhr-81	3.16
T19D12.4	leukocyte adhession glycoprotein	3.0
Y67A10A.1	integral membrane O-acyltransferase	3.0

Table 2.2. List of genes downregulated in *nhr-49-/-* compared to wildtype N2 animals. Values represent fold changes from average mRNA levels obtained from three independent biological replicates.

Table 2.2

Genepairs name	sequence description	fold change
F28F8.2	acs-2	25.6
F10D2.9	fat-7	16.2
K12G11.3	alcohol dehydrogenase	6.85
C17C3.12a	acdh-2	5.05
C45B11.3	dhs-18	4.63
F18E3.7a	D-aspartate oxidase	4.52
C32H11.12	dod-24	4.33
F18E3.7a	D-asparatate oxidase	3.94
Y10D10A.9	lectin	3.89
Y38E10A.15		3.25
T09F5.9	c-type lectin	3.24
F23C8.4	ubiquitin regulatory protein	3.23
F18E3.7a	D-aspartate oxidase	3.2
Y75B8A.4	mitochondrial ATP-dependent protease	2.99
C47F8.1	F-box protein	2.95
R09D1.7	chitinase	2.94
F48G7.3	nhr-83	2.93
F45C12.1	EGF receptor-like	2.92
C53A3.3	nitophenyl phosphatase	2.92
R13D11.1		2.85
C17C3.12b	acdh-2	2.85
Y34F4.2		2.82
C36A4.1	cyp-25a1	2.8
F53G2.1	centriolin serine threonine kinase	2.78
F09F3.9	cpt-5	2.78
F11A5.3	rab-2 GTPase	2.78
R08C7.8	serine threonine phosphatase	2.75

Table 2.3. List of candidate proteins identified using Yeast two hybrid analysis using NHR-49-LBD as bait.

Table 2.3

1. nhr-13	11. nhr-234
2. nhr-19	12. nhr-243
3. nhr-22	13. nhr-247
4. nhr-49	14. nhr-256
5. nhr-66	15. MDT-15
6. nhr-71	16. efl-1
7. nhr-76	17. lin-45
8. nhr-79	18. ttr-27
9. nhr-80	19. vab-1
10. nhr-105	20. F54A5.11
	21. F54D10.7

Table 2.4. List of forward primers used for qRT-PCR.

Table 2.4

Well	Oligo Name	Sequence (5' to 3')	Well	Oligo Name	Sequence (5' to 3')
A1	B0348.2	cagtgcaatcaagtgacacg	E1	C47F8.1	cttccaactccagcaactcc
A2	B0222.4	ttcacgagtttgctcacagc	E2	R09D1.7	acttccaccacctgatttgg
A3	F45E4.1	tgtttgtggtggacagttcg	E3	F48G7.3	aagccgcaggaacttttatcc
A4	R08H2.9	tgggctaaccatttgaacc	E4	F45C12.1	ccacctatcgaaggaaaacg
A5	Y65B4BR.1	cctccatgtgttccgagtgc	E5	C53A3.2	gaagaatcagttccccacttcc
A6	Y37H2A.11	aaggtccaagccaaaagagc	E6	R13D11.1	tcgagcatcatttgaattgc
A7	C29F3.5	atgggctcttttgtcaatgg	E7	Y34F4.2	tggttgacttgaagctctgc
A8	ZK218.5	caaggaggatgtgttgatgc	E8	C36A4.1	agatgtgattgggaaaatgtgc
A9	W03B1.6	tcacgcttcccttgtctacc	E9	F53G2.1	atacgtggattgcggtatgg
A10	ZK617.2	agaagggcttcggaattcacc	E10	F11A5.3	aagtgaagcttcgtgtttgg
A11	F27E5.1	cgtaccactgggaaaacttgg	E11	R08C7.8	tcacgaagtgtctcaggaagg
A12	E02H9.5	agctcttctcgctgaaatcg	E12	ZK265.1	cacgatgatctgcatcaacc
B1	T10B9.1	ggttgagaacattggcttcg	F1	Y73B6BL.11	gcttaacatgtgcgttgtgc
B2	C36C5.14	tgcatgaaacaggaggttacg	F2	M04C9.4	aatcgctgggagaaaatgc
B3	C29F3.2	ttggagatccttccatcagg	F3	C55A1.6	caagaaccgaagctgaagagtgc
B4	T24C4.4	actgatagctggcttgtttgg	F4	T03D3.1	aaacattgaatccgcttttgc
B5	F54F3.3	ccccttgaattgatggatgg	F5	C45E5.1	aactggaccccgatcataagg
B6	ZK218.3	gcaacagatgctcctcaacc	F6	K10C2.3	cactgttgtgatcggagacc
B7	Y46C8AL.4	cttgcgtcacagagcaaatgg	F7	ZK550.6	aaatggaaccccggagatacc
B8	C47F8.5	ccaggaggaatgttttgagg	F8	R106.2	ggccgctattgtgtacttcc
B9	C47A10.1	gtgggacctagtggttgtgg	F9	T05B4.3	ccaagacctgtggattctgc
B10	C04G6.5	tgaacgatggctacagatgc	F10	F19B10.2	ggcgaaaatgaccagaaagcc
B11	F35E8.8	cggaaaaacccccatacaacc	F11	C33F10.1	gcctcctcaactaaccatgc
B12	C47F8.8	tacttgagaaggaagatatgg	F12	K09H11.7	ttcatttttgacgctgatgg
C1	T19D12.4	ctgatgttttggcacagtcg	G1	K10C3.6a	tgccagcatttcgaagtccc
C2	Y67A10A.1	tacttcgcttttggattttgg	G2	fat-1	caccgctgaagagccgacgc
C3	F57B9.6	ctgtaacactcgcagagaagg	G3	fat-2	catacattgagcattatctccg
C4	ZK218.11	tccaatcatctccctcttgc	G4	gei-7a	cgcgtgctcagctctggc
C5	C18A11.1	caaagcttgaaaattgacatcg	G5	acs-2	caacaacgcatatttcgcagg
C6	Y73F8A.8	cagcttgtcagcagtcttgc	G6	NHR-23	cggatattctatagctgttgc
C7	F37B1.3	ttcccagttcgtggtctagc	G7	R09B5.6	tcaatttgtacggtggaagcg
C8	T16G1.6	aagccgtatgagttgcatcc	G8	K11D12.4	aactgctcgagatgtctcgc
C9	T24E12.5	ccaacttcgtgacgctaacc	G9	Y48G9A.10	aaggacgaacactacaacgc
C10	C54E4.5	tcaaaagtgagtgaaattcg	G10	F09F3.9	tcacactgaactgatcaagac
C11	F45D11.1	gacaagaaagcgaaggaacg	G11	F40F4.3	ctgattcttgttggagctgc
C12	C53B4.7b	gctgaagtagacgctgttgc	G12	T22G5.6	gtcttcttattcgtaaagctgc
D1	R52.6	tgccatatgaggagactacgg	H1	E04F6.5b	gacttctgacattccaaagagc
D2	W02B12.1	attttcaacgggattctgg	H2	fat-7	gctctctatgtgttctcagg
D3	ZC443.5	ggaaatatgaagaagccaatgc	H3	fat-5	cgagatccgacaaatgcagg
D4	K12G11.3	gatcacggaagcaaagaagc	H4	fat-6	cttctgtatgtgttcggagg
D5	C45B11.3	ctgctcatccaaaactaccg	H5	C29F3.1	gatatagcctctgtattttgctc
D6	F18E3.7a	tacggacgtgcttctttcg	H6	T05G5.6	aagcttggaatgctttgtgcg
D7	C32H11.12	ctcatcttggcatccttgc	H7	C55B7.4A	acaacatcagattgcacaagc
D8	Y19D10A.9	aactggagcttccgatatgc	H8	F28D1.9	agtggtactactggaatgcc
D9	Y38E10A.15	ctggaatcatccgtgatcg	H9	C02B10.1	gctgagtatggtggatctgg
D10	T09F5.9	tcgtgtaatgatgcagtttgc	H10	nhr-80	tttccacatttgggatctgg
D11	F23C8.4	caattccgacttctcgatgg	H11	nhr-80b	ccgatttccagcttcttcc
D12	Y75B8A.4	ctactgctggatgtgatcg	H12	nhr-66c	ctcacagcgacaatgactcc

Table 2.5. List of reverse primers used for qRT-PCR.

Table 2.5

Well	Oligo Name	Sequence (5' to 3')	Well	Oligo Name	Sequence (5' to 3')
A1	B0348.2	tggatgaatcacagcaaagc	E1	C47F8.1	aggctcttttttcacgagacg
A2	B0222.4	gaacaaccagcaggaagagg	E2	R09D1.7	gttgccccagttatcatttcc
A3	F45E4.1	ggcatatcctgcttgtttgc	E3	F48G7.3	atttgctggatgtcgtagcc
A4	R08H2.9	agccacactcctttgattcc	E4	F45C12.1	tgatgttcaccgaacacttgg
A5	Y65B4BR.1	gaatctcctgctgagcatcc	E5	C53A3.2	tctgcagtttggatcaagtcc
A6	Y37H2A.11	atctcggtgctcacaattcc	E6	R13D11.1	agagcaactgccatgaaacc
A7	C29F3.5	atgtgaaggaactgggatgg	E7	Y34F4.2	agtttgccagatgcttttcg
A8	ZK218.5	ctgcaacctccaatgattcc	E8	C36A4.1	gtgtcggatgtcaatgttcg
A9	W03B1.6	acctcgcatgacaatgtgg	E9	F53G2.1	agcgttgaagaacactgtcg
A10	ZK617.2	cttggaaagaccagcagtgg	E10	F11A5.3	ctgctccaagtgaacgaagg
A11	F27E5.1	cgaaaagctgtccaaagtcc	E11	R08C7.8	gctcgtaagaatccgagacg
A12	E02H9.5	gccttcctcgttgatagtcg	E12	ZK265.1	tttgcgacttcaactgattcc
B1	T10B9.1	cttttgcacttgcctcatcc	F1	Y73B6BL.11	actgccaaatggatctctcg
B2	C36C5.14	tcacacttgctgacgagtcc	F2	M04C9.4	tggcggagacttttcatagc
B3	C29F3.2	attcaggcgagaaaacttcg	F3	C55A1.6	gcgataaacttgtcggaagc
B4	T24C4.4	aataaccgggaagaacaaacc	F4	T03D3.1	tgtgtcgttcgccttatcc
B5	F54F3.3	ctttaagtccagcgcaaacc	F5	C45E5.1	gcggctttcatcagtttagg
B6	ZK218.3	gggcaggagtgtagaagtcg	F6	K10C2.3	aatcccaatcccaaaattcc
B7	Y46C8AL.4	tggaggaagcacttgaaacc	F7	ZK550.6	tgcgtagtgacaggagatcg
B8	C47F8.5	ctcgatagtcctccgacacc	F8	R106.2	gagacgactgggcaaatag
B9	C47A10.1	gatgtttcgggttcatttgg	F9	T05B4.3	gtgacagagtcgcattgagc
B10	C04G6.5	tcctggaagccagaagagc	F10	F19B10.2	cataatctccgcatcgttgc
B11	F35E8.8	gccaaggagttgacttgagc	F11	C33F10.1	gaggcttttgtgtgatttgg
B12	C47F8.8	tatcacctttgcgctttcc	F12	K09H11.7	gagatttgtgtggcattattgg
C1	T19D12.4	tcacgaactccggttactcc	G1	K10C3.6a	gttgtcgcattggccagac
C2	Y67A10A.1	tggcgcaaatctacaataacc	G2	fat-1	tagagaattgtgagtgccgc
C3	F57B9.6	gatcctgaacggaactctcg	G3	fat-2	cattgagccattcataatcgg
C4	ZK218.11	tcacgcaattagtcgcttcc	G4	gei-7a	gacaactgatccggctccg
C5	C18A11.1	caccatgcacacaaaatctcc	G5	acs-2	gggaagaccacagtttgtcc
C6	Y73F8A.8	agatggttgacattggactgg	G6	NHR-23	acttgtggcgatgggaagc
C7	F37B1.3	tcttctcccaggtgtcatcc	G7	R09B5.6	tttcctccaaggctgctgc
C8	T16G1.6	tcgtcgttgaacatcgtacc	G8	K11D12.4	agagtggatatcttccagcc
C9	T24E12.5	ttcgtggttgttgtctctcg	G9	Y48G9A.10	cgcattggcaggtactactc
C10	C54E4.5	agtttgcctcatccacatcc	G10	F09F3.9	gtagagcatatcgccctgc
C11	F45D11.1	cgccataatcactttgagagg	G11	F40F4.3	gtttacgagtgaaccatccg
C12	C53B4.7b	tacaattcggatgtggatgc	G12	T22G5.6	ctctctaattttgaaagcgagc
D1	R52.6	ctcctaattccaatgtccatcc	H1	E04F6.5b	acaatttcagcgactctggc
D2	W02B12.1	atatttccatgcccgtaagc	H2	fat-7	caatgatgtcattttgaaagagc
D3	ZC443.5	ctccattgtactgcccaacc	H3	fat-5	aacacaagctgatatagtccg
D4	K12G11.3	tcctccctcagtcaatttgc	H4	fat-6	gatgacgtcatttgaagagc
D5	C45B11.3	tttactgctgcctcatcacc	H5	C29F3.1	aattgtcctccactcttcac
D6	F18E3.7a	ccataggctctttgttgttgc	H6	T05G5.6	catctccttgatatcagctcc
D7	C32H11.12	agctctgtccatcccatcc	H7	C55B7.4A	gtgatgcaaacagtttcgcc
D8	Y19D10A.9	tagaaacctgcggagactgg	H8	F28D1.9	tgataaattggcatcgagacg
D9	Y38E10A.15	gtggaacttgaggcccatcc	H9	C02B10.1	ctcttcagatccatttctcac
D10	T09F5.9	ttagtcgaatctgcccaagc	H10	nhr-80	ttttcaagctttgcctgacc
D11	F23C8.4	atcctcggtgaacactttgc	H11	nhr-80b	acattgcagtcatcccttcc
D12	Y75B8A.4	tgcattctgattggagatgg	H12	nhr-66c	agttcaatccgtccagtctagc

Table 2.6

Name	ID	logFC	AveExpr	P.Value	function
ZK218.5	cea2.i.48948	7.10	7.40	1.81E-09	secreted surface protein
F56H6.5	cea2.i.03172	5.59	7.26	4.69E-09	GDP mannose dehydratase
B0222.4	cea2.i.31956	5.27	7.86	3.21E-08	tag-38, sphingosine phosphate lyase
F41D3.11	cea2.i.02605	4.06	6.39	0.00000714	glycosyltransferase
Y65B4BR.1	cea2.i.06720	4.01	6.59	0.000000473	phospholipase
ZK617.2	cea2.i.31736	3.96	9.27	2.79161E-06	tag lipase
F56H6.1	cea2.i.03125	3.94	5.15	0.035191188	galactosyltransferase
F56H6.11	cea2.i.03134	3.77	5.13	0.035304876	integral membrane O-acyltransferase
Y46C8AL.4	cea2.i.30277	3.42	6.26	0.000319317	c-lectin
B0348.2	cea2.i.32048	3.28	8.58	1.49225E-06	
Y67A10A.1	cea2.i.06753	3.18	8.33	4.17979E-08	integral membrane O-acyltransferase
F46B3.7	cea2.i.39241	3.16	5.84	0.02183245	
T26E4.9	cea2.d.08064	3.11	6.36	0.000773916	
T26E4.10	cea2.d.08063	2.95	5.86	0.004450069	
F56H6.7	cea2.i.03190	2.90	5.62	0.005213923	
C53B4.7b	cea2.d.01787	2.85	6.85	3.37005E-06	bre-1
B0554.4	cea2.i.32177	2.56	6.32	5.38644E-06	
F11A5.5	cea2.i.36289	2.45	7.23	4.40064E-07	predicted glycosyltransferase
Y46C8AL.2	cea2.i.30269	2.43	7.34	1.5938E-06	c-lectin
F57E7.1	cea2.d.29913	2.36	6.33	1.00499E-05	
T28C6.6	cea2.d.40651	2.25	13.75	0.036004092	col-3
K11H12.4	cea2.i.27460	2.23	8.27	3.31344E-06	
F38H12.3	cea2.i.38647	2.22	7.39	8.30508E-07	nhr-181
F27E5.1	cea2.i.11595	2.20	9.08	5.10014E-06	acid ceramidase
F11A5.8	cea2.i.36313	2.12	5.98	0.003181542	O-acyltransferase homolog
F08F8.5	cea2.p.158384	2.10	6.97	1.06924E-06	numr-1 nuclear localized metal responsive
F58B3.2	cea2.d.30172	2.06	9.30	8.44982E-05	lys-5
F41D3.1	cea2.i.02594	2.05	5.64	0.00177113	nhr-82
B0454.8	cea2.i.08369	2.02	7.42	1.70699E-05	
T20D4.7	cea2.d.39379	1.96	6.27	0.000296875	thioredoxin
C07G3.2	cea2.i.32798	1.93	6.80	3.61822E-05	irg-1 infection responsive gene
Y73F8A.9	cea2.d.47046	1.85	9.38	0.000237431	pqn-91
E02H9.5	cea2.3.07963	1.80	6.10	0.000396968	klo-2 beta-glucosidase
ZK1010.7	cea2.c.25574	1.76	11.29	0.003609609	col-97
F13E9.8	cea2.p.90496	1.68	6.93	0.000554869	
Y73F8A.9	cea2.d.47041	1.67	8.07	0.000444577	pqn-91
W02B12.1	cea2.p.48441	1.62	9.38	3.40121E-05	phospholipase
Y105C5A.4	cea2.d.41903	1.61	9.58	0.000217985	pqn-77
Y39G10AR	cea2.p.20677	1.56	6.66	0.001941983	ugt-31 UDP-glucuronosyltransferase
ZK666.7	cea2.c.15765	1.54	6.88	0.003833373	c-lectin
T19D12.4	cea2.p.47251	1.52	9.64	2.12179E-05	
F45D11.14	cea2.d.26120	1.52	7.05	0.040389476	
R12E2.14	cea2.p.158399	1.51	11.57	0.000272437	
T06E4.10	cea2.i.43867	1.48	5.72	0.001316791	

Table 2.7. The top downregulated genes in *nhr-66-/-* animals. Genes are ordered by highest statistical significance of underexpression in *nhr-66-/-* animals vs control N2 animals. The data represent the output of "limma" analysis from three independent mRNA isolations and microarray hybridizations. "ID" refers to the identity of individual spots on the arrays, "logFc" represents the log of the fold change, "AveExpr" represents the averaged spot intensity and "Function" refers to the predicted or actual function according to Wormbase.

Table 2.7

Name	ID	logFC	AveExpr	P.Value	function
T05B4.3	cea2.c.38150	-5.92	7.28	6.044E-08	phat-4
C49G7.3	cea2.d.17457	-3.99	6.80	0.0034499	secreted surface protein
ZK1025.3	cea2.i.07449	-3.85	7.74	0.0001157	predicted small mol methylase
T27E4.4	cea2.c.38832	-3.44	9.52	4.047E-06	fip-2
C49G7.4	cea2.c.50260	-3.32	5.62	0.0009528	phat-3
ZK1025.5	cea2.d.48138	-2.34	6.65	2.844E-05	
C29F3.5	cea2.i.33937	-2.27	6.77	0.0002765	c-lectin
C27C7.4	cea2.d.14567	-2.14	6.23	0.0015523	nhr-73
ZK1025.10	cea2.d.48121	-2.07	5.99	0.0052083	nhr-245
T09A12.4c	cea2.d.38246	-2.06	4.98	0.0200565	nhr-66
T05B4.9	cea2.d.37120	-2.00	6.07	0.038735	secreted surface protein
C27C7.4	cea2.d.14568	-1.85	5.87	0.000437	nhr-73
C27C7.8	cea2.d.14571	-1.72	5.60	9.75E-05	nhr-259
F38A3.1	cea2.p.39129	-1.61	8.44	0.0386752	col-81
ZK1025.6	cea2.d.48143	-1.53	7.68	3.526E-05	nhr-244

Table 2.8. List of top upregulated genes in *nhr-80-/-* worms compared to wildtype worms. Genes are ordered by highest statistical significance of overexpression in *nhr-80-/-* animals vs control N2 animals. The data represent the output of "limma" analysis from three independent mRNA isolations and microarray hybridizations. "ID" refers to the identity of individual spots on the arrays, "logFc" represents the log of the fold change, "AveExpr" represents the averaged spot intensity and "Function" refers to the predicted or actual function according to Wormbase.

Table 2.8

Name	ID	logFC	AveExpr	P.Value	
C26F1.9	cea2.c.34189	3.30	12.25	0.00118939	rpl-39
K02F2.2	cea2.c.04646	2.18	13.47	0.00417723	ahcy-1
F59D8.2	cea2.3.17694	2.11	10.12	0.00276135	vit-4
C04F6.1	cea2.d.10603	2.01	10.91	0.00102914	vit-5
F59D8.1	cea2.d.30363	2.00	10.95	0.00135702	vit-3
B0412.4	cea2.c.16346	1.86	13.50	0.00081612	rps-29
M18.1	cea2.p.96223	1.74	11.17	0.0114384	col-129
C42D8.2	cea2.p.158069	1.69	10.78	0.00265827	vit-2
F55B11.2	cea2.p.93808	1.68	7.52	0.0048175	
F26F12.1	cea2.p.115085	1.66	8.47	0.02553253	col-140
F41F3.4	cea2.p.116685	1.64	9.26	0.01851528	col-139
Y62H9A.6	cea2.c.48585	1.63	7.79	0.00968345	
F54E7.2	cea2.c.19871	1.62	12.40	9.37E-05	rps-12
K01G5.7	cea2.c.21122	1.60	12.58	0.00049039	tbb-1
ZC373.2	cea2.p.156987	1.54	7.93	0.00271114	
F11G11.11	cea2.p.36165	1.50	8.85	0.00962828	
C23G10.3	cea2.c.17471	1.49	11.63	0.02217814	rps-3
C44B12.1	cea2.p.87992	1.49	9.02	0.00125503	
F59D8.1	cea2.d.30360	1.46	9.22	0.02460609	vit-3
T21G5.3	cea2.c.06057	1.46	11.11	0.00036855	glh-1
D1054.10	cea2.c.34996	1.44	9.27	0.01935949	
K07H8.6	cea2.p.95377	1.44	9.98	0.00696731	vit-6
ZK1193.1	cea2.c.49373	1.43	9.33	0.03410419	col-19
Y37D8A.19	cea2.c.23704	1.42	8.07	0.01382848	
F02A9.3	cea2.d.01994	1.42	14.28	0.03509986	far-2
W02D9.7	cea2.p.18814	1.40	6.84	0.02354035	

Table 2.9

Table 2.9 lists the top downregulated genes in *nhr-80-/-* animals. Genes are ordered by highest statistical significance of underexpression in *nhr-80-/-* animals vs control N2 animals. The data represent the output of "limma" analysis from three independent mRNA isolations and microarray hybridizations. "ID" refers to the identity of individual spots on the arrays, "logFc" represents the log of the fold change, "AveExpr" represents the averaged spot intensity and "Function" refers to the predicted or actual function according to Wormbase.

Name	ID	logFC	AveExpr	P.Value	
F10D2.9	cea2.c.35201	-5.55	8.18	5.11E-08	fat-7
ZC395.5	cea2.i.22724	-2.59	8.64	0.000613	4
ZK666.7	cea2.c.15765	-2.37	6.64	0.010779	5 c-lec
ZK666.6	cea2.i.18053	-2.23	8.61	7.33E-05	c-lec
W06D12.3	cea2.c.39182	-2.17	8.62	1.58E-06	fat-5
C45G7.3	cea2.d.16969	-2.16	6.74	0.000841	2 ilys-3
C53A3.2	cea2.i.35082	-2.05	7.99	0.000481	8 p-nitrophenyl phosphatase
F38E11.1	cea2.i.25955	-1.81	8.35	6.65E-06	hsp-12.3
T09F5.9	cea2.p.124403	-1.75	11.13	3.49E-06	c-lec
K09H11.7	cea2.d.33151	-1.73	10.59	7.59E-05	p-nitrophenyl phosphatase
C50F7.5	cea2.p.88996	-1.49	6.79	0.026963	2
F49E11.10	cea2.c.28925	-1.48	10.19	0.019819	1 scl-2
F15E11.1	cea2.d.20845	-1.46	12.26	0.000935	9
K12G11.3	cea2.c.37571	-1.41	12.44	0.013320	2 sodh-1
Y119D3B.9	cea2.i.21452	-1.38	6.88	0.014627	8 fbxa-21
F53A9.8	cea2.c.45618	-1.38	10.60	0.001478	6
VZK822L.1	cea2.c.31436	-1.29	11.00	2.85E-05	fat-6
Y34F4.2	cea2.p.75989	-1.29	5.80	0.000565	2
H10E21.3a	cea2.d.30973	-1.29	8.76	0.001102	6 nhr-80
C02A12.4	cea2.p.107596	-1.28	9.59	0.010821	7 lys-7
Y51A2D.4	cea2.p.129201	-1.26	7.27	0.001375	4 hmit
C44C1.6	cea2.c.42196	-1.23	7.45	0.007966	5
F54B11.11	cea2.i.54612	-1.20	9.09	9.18E-05	

Table 2.10

Table 2.10. Summary of gene expression data using qRT-PCR on *nhr-49-/-*, *nhr-66-/-*, *nhr-80-/-* and *nhr-13-/-* animals with respect to wildtype controls. Values represent fold change +/- SEM of *nhr-49-/-*, *nhr-66-/-*, *nhr-80-/-* and *nhr-13-/-* normalized to wildtype levels.

Gene name	Gene	Overall fold change with respect to wildtype			
		nhr-49-/-	nhr-66-/-	nhr-80-/-	nhr-13-/-
acid ceramidase	F27E5.1	2.29+/-0.7	2.29+/-0.5	1+/-0.6	1.7+/-0.5
glycosylhydrolase	E02H9.5	4+/-1.17	4+/-1.5	0.5+/-0.2	0.5+/-0.2
sphingosine phosphate lyase (SPL)	B0222.4	32+/-12.3	16+/-5.44	0.2+/-0.2	0.2+/-0.2
phospholipase	Y65B4BR.1	8+/-3.4	4+/-2.2	0.2+/-0.2	0.4+/-0.4
phospholipase	W02B12.1	2+/-0.5	2+/-0.3	0.3+/-0.1	0.4+/-0.1
TAG lipase	ZK617.2	32+/-9.3	16+/-6.1	1+/-0.4	1.7+/-1
O-acyltransferase	Y67A10A.1	4+/-1.36	8+/-2.7	0.5+/-0.6	1+/-0.7
fat-7	F10D2.9	128+/-53	1+/-0.3	128+/-40	73.5+/-16.9
fat-5	W06D12.3	16+/-2.4	1+/-0.1	8+/-5.9	2.14+/-0.8
fat-6	VZK8221.1	2+/-0.4	1+/0.3	4+/-1.2	1.5+/-0.3

Table 2.11

Table 2.11. Summary of lifespan data. SEM: standard error of the mean. The 50th percentile is the age when the fraction of animals alive reaches 0.5. The number of animals is the sum of assayed worms per strain from atleast 4 independent experiments.

Strain	mean+/-SEM (days)	50th percentile (days)	no. of animals	p-value (compared to N2)
WT	17.35+/-0.34	18	195	N/A
nhr-49 (nr2041)	9.52+/-0.23	9.5	139	<0.0001
nhr-66 (ok940)	17.16+/-0.41	17	96	ns (0.73)
nhr-80 (tm1011)	13.19+/-0.38	12.5	129	<0.0001
nhr-13 (vc1656)	14.17+/-0.4	13	135	<0.0001
nhr-80;nhr-13	12.29+/-0.37	11	139	<0.0001

Table 2.12

Table 2.12. Lifespan and relative C18:0 fatty acid abundance. Mean lifespan +/- SEM numbers represent the combined average of atleast four experiments. Fatty acid abundance is indicated by percent of total fatty acid measured by GC/MS. The percent of C18:0 and C18:1n9 shown is the result of four independent experiments.

		% of total fatty acids		
Strain	mean lifespan	C18:0	C18:1n9	ratio
WT	16.7+/-1.5	4.98+/-0.15	5.14+/-0.22	0.98+/-0.06
nhr-49 (nr2041)	9.5+/-0.4	8.97+/-0.62	2.46+/-0.39	3.74+/-0.33
nhr-66 (ok940)	16.9+/-0.4	5.68+/-0.35	5.23+/-0.49	1.09+/-0.04
nhr-80 (tm1011)	13.3+/-0.7	8.63+/-0.48	3.6+/-0.17	2.4+/-0.22
nhr-13 (vc1656)	14.3+/-1.4	5.27+/-0.24	5.46+/-0.13	0.96+/-0.02
nhr-80;nhr-13	12.17+/-0.8	9.74+/-0.33	3.32+/0.27	2.99+/-0.22

Table 2.13. Insights on evolution

Table 2.13

NRs	Physiological role	metabolic pathways	structure	
Mammals			**homo**	**hetero**
HNF-4α	liver differentiation, nutrient transport, lipid metabolism, xenobiotic metabolism, glucose metabolism, amino acid metabolism, blood maintenance, immune function		X	
PPAR-α/ RXR	lipid metabolism, cholesterol metabolism, glucose metabolism fasting response	beta-oxidation, gluconeogenesis		X
Drosophila				
dHNF-4	lipid transport, lipid metabolism, fasting response, gut differentiation	beta-oxidation, gluconeogenesis	X	
C. elegans				
NHR-49	lipid metabolism xenobiotic metabolism, fasting response	beta-oxidation, fatty acid desaturation, regulation of sphingolipid and lipid remodeling genes, P450, gluconeogenesis	X	X
NHR-66	lipid metabolism	regulation of sphingolipid and lipid remodeling genes	?	X
NHR-80	lipid metabolism	fatty acid desaturation	?	X
NHR-13	lipid metabolism	fatty acid desaturation	?	X
Yeast				
OAF-1/PIP2	lipid metabolism			X

CHAPTER 3

ROLE OF NHR-49 IN REGULATING THE GLOBAL "LIPID ECONOMY"

Abstract

Mammalian nuclear receptors broadly impact metabolism. This regulation is often complex, involving the intersection of multiple receptors to regulate metabolic homeostasis in multiple organs. Therefore the ability to integrate a clear picture of each nuclear receptor and targets' function has not been possible. Here, capitalizing on the advantages of *C. elegans*, we have been able to illustrate the functions of NHR-49 as a global regulator of energy availability and reproduction. Ultrastructural analysis suggests that NHR-49 and its co-factors participate in the regulation of nutrient stores in the intestine and hypodermis. We also observe a reduced brood size and reduced mitotic region in the germline of *nhr-49-/-* animals suggesting a link between nutrient stores and reproduction. We also show a surprising difference between the kinetics of energy storage and utilization in the intestine versus the hypodermis, with the intestine being more responsive to short term changes in nutrient intake, whereas the hypodermis functions as a more stable long term lipid storage tissue. Collectively, our data suggests that nuclear receptors have the ability to sense global supply and demand in a "lipid economy".

Introduction

Energy homeostasis is maintained by an extremely complex network of signaling pathways that operate in multiple tissues and that can mediate different aspects of energy balance, including nutrient uptake, storage of resources and energy expenditure. For these processes to occur effectively, mechanisms have evolved to sense nutrients and coordinate various activities between different tissues (Jones and Ashrafi 2009). Impairments in any of these functions is detrimental as not only does nutrient insufficiency starve important tissues, but the over supply of nutrients also needs to be recognized and delivered to short-term inventories or long-term reserves. Nutrient excess for example, contributes to metabolic disease, at least in part, when distribution mechanisms are no longer able to appropriately handle excess products. For example, pathologically high levels of lipids can overwhelm adiposity storage mechanisms, resulting in the overflow of lipids to cells and organs not readily-equipped to take on this surplus, like the heart and liver (Schaffer 2003). Therefore, in order to avoid catastrophic imbalances, organisms have developed various mechanisms for monitoring the supply and demand of various nutrient resources.

Nuclear receptors are perhaps the most notable examples of these, responding to small molecule hormones or metabolites that direct a diverse set of biological mechanisms and in many cases, also exacerbate or mitigate associated diseases. For the metabolic syndrome, which involves imbalances in energy homeostasis, the lipid sensing nuclear receptors are key players. By binding to fatty acids ligands, these receptors can globally execute transcriptional programs that control all aspects of lipid metabolism, including storage, expenditure, and trafficking (Chawla, Repa et al. 2001; Evans, Barish et al. 2004).

The PPAR and HNF4 are widely-studied examples of nuclear receptors that help control the supply and demand of various fatty acids, by sensing lipid composition in numerous tissues in the body (Evans, Barish et al. 2004). This is especially important as lipids are sourced from multiple locations, including diet, *de novo* synthesis, macromolecular breakdown, and have to be distributed to perform various tasks, such as fuel storage, organismal structures, and vesicular trafficking. Nuclear receptors serve not

only to distribute and deliver their commodities in favorable conditions, but also have to determine what activity is most relevant and needed, in adverse conditions.

Nuclear receptors have been shown to run the gamut from sensing the environment for signals to responding to them by regulating appropriate target genes. For example, during times of starvation, PPARs activate genes in the beta-oxidation pathway so that fatty acids can be oxidized to generate energy; however, how nuclear receptors co-ordinate the distribution and delivery of fatty acids that are needed to perform their different jobs, is still not known (Kersten, Seydoux et al. 1999; Leone, Weinheimer et al. 1999). Another layer of complexity is that nuclear receptors utilize various types of co-factors that not only help turn on and off binary responses, but also enable receptors to differentially regulate subsets of genes depending on specific conditions (Perissi and Rosenfeld 2005).

Invertebrate models often provide excellent opportunities to bridge the gap in knowledge left by studies focusing on physiological phenotypes and transcriptional regulatory complexes. *C. elegans* has already been fruitful for the identification of dozens of novel genes and pathways involved in fat storage and metabolism, many of which have been confirmed in mammalian models (Ashrafi, Chang et al. 2003; Jones, Greer et al. 2009). For study of lipid sensing nuclear receptors, NHR-49 stands out as a good candidate because it has already been shown to regulate lipid metabolism gene patterns similar to that of PPAR and HNF4; with similar overall effects on fat storage and also a critical role in the fasting response, showing common environmental sensing capacity and downstream outputs. Thus, we set out to test the hypotheses alluded to above that lipid sensing nuclear receptors would be adept at precisely coordinating various inputs and outputs in order to regulate lipid homeostasis in response to multiple environmental pressures. Nuclear receptors often respond differently to the same lipophilic ligand in different tissues. We wanted to examine the influence of NHR-49 on energy storage in different tissues of the worm. We chose to look at the intestine and hypodermis, the primary sites of *C. elegans* fat storage and metabolism to test this hypothesis and its predictions.

Results

Overall nutritional reserves in the intestine and hypodermis are reduced in *nhr-49-/-* animals

We analyzed serial section of *C. elegans* using high pressure-transmission electron microsopy (HP-TEM) and quantitatively measured fat stores in the intestine and the hypodermis. We observed two distinct types of fat structures: (1) mono-layered lipid droplets that primarily store fat and are typically seen in the intestine and hypodermis and (2) multi-layered chylomicrons or yolk vesicles that transfer lipoproteins from intestine to oocytes. We measured the average fractional area occupied by lipid droplets in the intestine of adult day one *nhr-49 (nr2041)* animals relative to the age matched wildtype animals. We found that *nhr-49-/-* animals had a significantly reduced intestinal lipid droplet fractional area compared to that of wildtype animals. Another interesting difference was that morphologically the intestinal lipid droplets in *nhr-49-/-* animals had a "collapsed membrane" which was not observed in wildtype animals (figures 3.1A and 3.1B). Even though, we did not observe any difference in the fractional area occupied by yolk droplets between *nhr-49-/-* and wildtype animals, we noticed that yolk droplets appeared morphologically different in appearance (figures 3.2A and 3.2B).

We next compared the average size of the hypodermis in wildtype and *nhr-49-/-* animals. We observed that *nhr-49-/-* animals had an average hypodermal area that was about three times smaller than that of wildtype animals (figure 3.3). Just like in the intestine, we quantified the lipid droplets in the hypodermis of adult day one *nhr-49-/-* mutants relative to the same aged wildtype animals. We observed that the hypodermal lipid droplets were significantly smaller in size in *nhr-49-/-* animals compared to wildtype animals (figure 3.4). In addition to lipids, another source of fuel utilized by *C. elegans* is the sugar glycogen. The nematode hypodermis is one of the primary sites of glycogen storage. We observed that adult day one *nhr-49-/-* mutants have depleted glycogen content in their hypodermis compared to wildtype animals (figures 3.5A and 3.5B).

Taken together, these results suggested that day one *nhr-49-/-* animals had reduced nutritional reserves compared to same aged wildtype animals as measured using serial HP-TEM images obtained from the intestine and hypodermis.

Co-factor partners participate in NHR-49's role in the overall nutritional reserves in the intestine and hypodermis

We had shown (chapter 2) that NHR-49 physically binds to NHR-66 and NHR-80 and they also have overlapping gene expression patterns. To test if NHR-49 partners, NHR-66 and NHR-80 contribute to the observed *nhr-49-/-* phenotypes, we examined adult day one *nhr-66 (ok940)* and *nhr-80 (tm1011)* deletion mutants. Like *nhr-49-/-* animals, *nhr-66-/-* animals also had significantly reduced fractional area of intestinal lipid droplets, but had wildtype amounts of fractional area of yolk droplets (figures 3.1B and 3.2B). In addition, the size of the hypodermis of these mutants was comparable to wildtype animals (figures 3.3 and 3.4). And finally, the amount of glycogen in these animals was similar to that of wildtype animals (figure 3.5). Based on these observations, we hypothesized that NHR-66 together with NHR-49 might be playing a role in the regulation of the amount of intestinal lipid droplets.

On the other hand, *nhr-80-/-* animals showed no significant difference in the fractional area of both intestinal lipid droplets and yolk droplets compared to wildtype animals (figures 3.1 and 3.2). Interestingly, *nhr-80-/-* animals had morphologically bigger and denser yolk droplets than wildtype yolk droplets. However, the hypodermal area of *nhr-80-/-* animals was significantly smaller than that of wildtype animals and also had comparatively reduced glycogen levels (figures 3.3 and 3.5). These observations seemed to imply that NHR-80 might be working with NHR-49 to regulate glycogen levels in the hypodermis.

Our findings thus far, support the notion that NHR-49 and its co-factors contribute to the regulation of different nutritional reserves in different tissues. Namely, NHR-49 together with NHR-66 might play a role in regulating the quantity of lipid

droplet levels in the intestine and NHR-49 together with NHR-80 might be contributing to glycogen levels in the hypodermis. In fact, *nhr-66-/-; nhr-80-/-* animals also had reduced fractional area of intestinal lipid droplets (figure 3.1) and reduced hypodermal glycogen (figure 3.5) further strengthening this model (figure 3.6).

Reduced fertility in *nhr-49-/-* animals

In *C. elegans*, the energetic requirements of reproduction are very high and fats are processed and mobilized to the germline. Since *nhr-49-/-* animals have reduced nutritional stores, we wanted to determine if reproduction or production of germ cells would be affected in *nhr-49-/-* animals. To determine if a full complement of germ cells developed, the number of embryos produced was counted. We thus measured the brood size of *nhr-49-/-*, *nhr-66-/-*, *nhr-80 -/-* and *nhr-66-/-;nhr-80-/-* animals. By counting the embryos of single animals, we found that *nhr-49(nr2041)* mutants produced an average of 140 +/- 11 eggs per adult worm and *nhr-80(tm1011)* animals produced an average of 181.75 +/- 9.4 eggs per adult worm compared with an average of 291.2 +/- 8.55 eggs for wildtype and 256.4 +/- 6.9 for *nhr-66(ok940)* animals. Furthermore, *nhr-66-/-;nhr-80-/-* animals that also have reduced lipid and glycogen stores also mirror the reduced brood size (102.1+/-10.3) observed in *nhr-49-/-* animals (figure 3.7). The reduced brood size seen in *nhr-49-/-* and *nhr-66-/-;nhr-80-/-* animals supports the idea that low reserves of lipid and glycogen might ultimately influence reproductive demand and result in a reduced number of progeny.

Reduced mitotic region in *nhr-49-/-* germline

It has been reported that in *C. elegans*, many more mitotic divisions are required for the production of a full brood than are needed for the development and growth to an adult. We reasoned that the one of the reasons we observe reduction in brood size might be a consequence of reduced mitotic divisions in the germline of *nhr-49-/-* animals. To test this, we stained extruded gonads of wildtype and *nhr-49-/-* animals with DAPI to stain the germ cell nuclei. We compared the total number of germ cells and the mitotic

region of wildtype and *nhr-49-/-* animals. The mitotic region extends from the distal tip of the germline tissue to the distal border of the transition zone in DAPI-stained germlines, transition nuclei are easily distinguished by their crescent shaped chromatin. Indeed, we did observe a noticeable reduction in total number of germ cells and the mitotic zone in day one *nhr-49-/-* animals compared to wildtype controls (data not shown) suggesting that there might be a link between energy storage, reproduction and germ cells.

C. elegans lipid stores are dynamic

C. elegans energy reserves are expected to be utilized during periods of food deprivation. We hypothesized that if we limited the nutritional reserves of the animal for a period of starvation, we might see a quantitative difference in lipid droplets in the intestine and hypodermis. We starved adult day one wildtype and *nhr-49-/-* animals for 15 hours and then quantified their intestinal and hypodermal lipid droplets. We observed that about half of the intestinal lipid droplets were used up by starved wildtype animals, whereas almost all of the intestinal lipid droplets were used up by starved *nhr-49-/-* animals, presumably because they had smaller reserves of intestinal lipid droplets to begin with (figure 3.8). Interestingly, we did not observe any yolk droplets in the intestine of the starved animals.

We did not observe any significant difference in the fractional area of lipid droplets in the hypodermis compared to the non-starved controls (figure 3.9 B). This suggested to us that the intestine might be the primary site for short-term storage whereas the hypodermis could be the site for long-term storage. Interestingly, starvation also reduced the size of the hypodermis in both wildtype and *nhr-49-/-* animals (figure 3.9A).

Discussion

Our study has shown for the first time that nuclear receptors are critical for maintaining proper nutrient stores in the intestine and hypodermis. Our data also suggests

that downstream physiological demands, like brood size are possibly affected as a result of the availability of accessible nutrients. We have demonstrated that wildtype levels of NHR-49 and its partner co-factors NHR-66 and NHR-80 are required for global energy stores and reproduction. We also demonstrate that the intestine and hypodermis might have different effects on utilization of stored lipids.

We observed that *nhr-49-/-* animals have overall diminished energy stores that included the amount of lipid droplets in their intestine and glycogen in their hypodermis relative to wildtype animals. In addition, our original microarray analysis revealed that NHR-49 broadly targeted functional groups that included genes involved in lipid binding, endo and exocytotic trafficking and egg yolk transfer. Therefore, it was not surprising that mutants defective in NHR-49 would have defects in different facets of lipid distribution and trafficking. Also, even though we do not observe any difference in the fractional area of yolk droplets in *nhr-49-/-* animals compared to wildtype, we observe morphologically different yolk droplets in *nhr-49-/-* animals. Taken together, *nhr-49-/-* animals not only have reduced amounts of lipid and glycogen in their intestine and hypodermis, they might also have oocytes defective in yolk uptake. The diminished supply of nutrients in the intestine, hypodermis and oocytes in *nhr-49-/-* animals could all be contributing to the observed reduced brood size. In support of the relationship between fat stores and fertility, *fat-6; fat-7* animals that have reduced fat stores also have reduced brood size compared to wildtype (Liang, Ferguson et al. 2010). Indeed, this "cost of reproduction" is thought to result from multiple processes competing for the same resources. That is, as the demands for offspring production increase, there are fewer resources available for somatic maintenance and repair, growth and movement (Partridge, Gems et al. 2005). Interestingly, in *Drosophila*, increased nutrient availability drives an increase in reproductive activity (Piper, Skorupa et al. 2005). Our data fits this concept, whereby *nhr-49-/-* animals have reduced nutritional reserves and a reduced brood size. Since most of the resources are used up for progeny production, there might be fewer resources available for somatic maintenance resulting in the shortened lifespan of *nhr-49-/-* (data shown in chapter 2).

Our work also demonstrates that NHR-49 along with its co-factors NHR-66 and NHR-80 regulate the total energy dynamics in *C. elegans* intestine and hypodermis. While a number of gene inactivations have been identified that alter *C. elegans* fat content, the molecular mechanisms that underlie regulation and distribution of global lipid stores is not known. Our data implies that deletions in NHR-49 and NHR-66 alter the amount of intestinal lipid droplets, whereas deletions in NHR-49 and NHR-80 reduce the amount of glycogen in the hypodermis. Extending this observation further, we speculate that NHR-49 and its partner proteins coordinate the supply of different types of fuel like lipid and glycogen from different tissues like intestine and hypodermis to be delivered to other tissues like oocytes and germline where they are utilized to meet different physiological demands. Additionally, our brood size data suggests that reduced supply of total energy stores is reflected in a smaller number of progeny. Preliminary data also suggests that the reduced brood size correlates with a reduced mitotic region in the germline. In fact, *nhr-66-/-;nhr-80-/-* animals which also have compromised levels of lipid droplets and diminished levels of glycogen have significantly reduced brood size, as well. These observations led us to speculate that NHR-49 and its partners not only regulate the coordination of fuel to different centers of supply, but further play a role in allocating these resources to the centers of demand.

Since both the *C. elegans* NHR-49 and the mammalian PPARs regulate similar metabolic pathways and physiological processes, we can conjecture that our findings are relevant in mammalian systems. In addition to enzymatic activities of lipases, the flux of stored lipids through fatty acid beta-oxidation might also be dependent on nuclear receptor regulated coordination and delivery of lipids from multiple fat storage depots. In conclusion, metabolic demands are dynamic and therefore a need to constantly monitor global energy levels is critical. Our work implies that nuclear receptors have the capacity to do exactly that, which is to sense both the supply and demand of nutrients to globally regulate lipid homeostasis.

Materials and methods

Nematode strains and growth conditions

C. elegans strains N2-Bristol (wildtype), *nhr-49* (nr2041), *nhr-66* (ok940), *nhr-80* (tm1011) and *nhr-66-/-;nhr-80-/-* were used for all experiments. Worms were maintained by standard techniques at 20°C. Single-worm PCR was used to determine the genotype of worms during crossing to generate *nhr-66-/-; 80-/-* double-mutant lines. For mRNA and GC/MS analysis, worm embryos were allowed to hatch on unseeded nematode growth media (NGM)-lite plates overnight at 20 °C. The next day, synchronized L1 larvae were plated onto NGM-lite plates seeded with Escherichia coli strain OP50. Worms were grown to early L4s at 20°C, harvested, washed three times with M9, and flash-frozen in liquid nitrogen.

High Pressure Transmission Electron microscopy

Day one adults were placed into a 20% BSA/PBS buffer solution and prepared in a Leica-Impact-2 high-pressure freezer according to the following protocol: 1) 60 hours in 100% acetone and uranyl acetate at –90°C. 2) Temperature was ramped from –90°C to –25°C over the course of 32.5 hours. 3) Next, sample was incubated at –25°C for 13 hours. 4) Next, the temperature change was brought from –25°C to 27°C in a 13 hour temperature ramp. Serial sections were post-stained in uranyl acetate followed by lead citrate. Thin cross sections were taken from resin-embedded clusters of young adults. Sections for adult animals were obtained from atleast 2 different animals.

Quantification of energy stores in different organs

Ten micron transverse sections typically spanning the length of the worm from the pharynx to the embryos were examined per animal. Lipid droplets, yolk and glycogen, intestine and hypodermis from every individual section were outlined and the average measurements were obtained using Image J software. Atleast two animals were

examined per mutant strain. Statistical data including p-values from one-tailed t-test were generated using GraphPad Prism Version 5 Software (GraphPad Software, San Diego, California, USA)

DAPI staining

Extruded gonads were fixed with methanol and rehydrated with phosphate-buffered saline (PBS) at room temperature. Worms were mounted and stained with DAPI and Vectashield. Confocal images were taken and analyzed.

Brood size

Synchronized L4 animals were placed on individual plates and brood analysis was performed by transferring the animals to fresh plates each day and counting the laid embryos and hatched L1 larvae 24 hours later. Statistical data including p-values from two-tailed t-test were generated using GraphPad Prism Version 5 Software (GraphPad Software, San Diego, California, USA).

Fig. 3.1

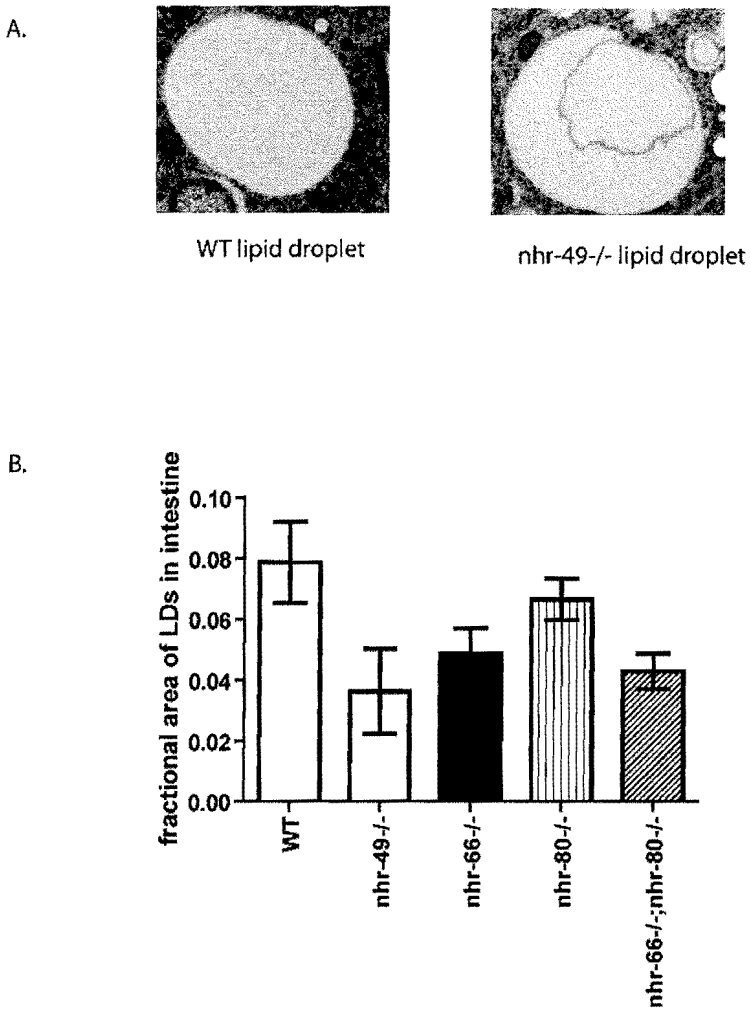

Fig 3.1. Quantification of lipid droplets in *nhr-49-/-* and its partner co-factors in *C. elegans* intestine.
A. High pressure freezing transmission electron microscopy (HP-TEM) images of intestinal lipid droplets in WT and *nhr-49-/-* animals.
B. The bar graph represents the mean (+/-SEM) fractional area of lipid droplets in the intestine of WT (white bar), *nhr-49-/-* (grey bar), *nhr-66-/-* (black bar), *nhr-80-/-* (vertical stripes bar) and *nhr-66-/-;nhr-80-/-* (slanted bar) animals. Atleast two animals were examined per mutant strain. p-value (compared to WT) < 0.05 (significant) for *nhr-49-/-*, *nhr-66-/-* and *nhr-66-/-;nhr-80-/-*.

Fig. 3.2

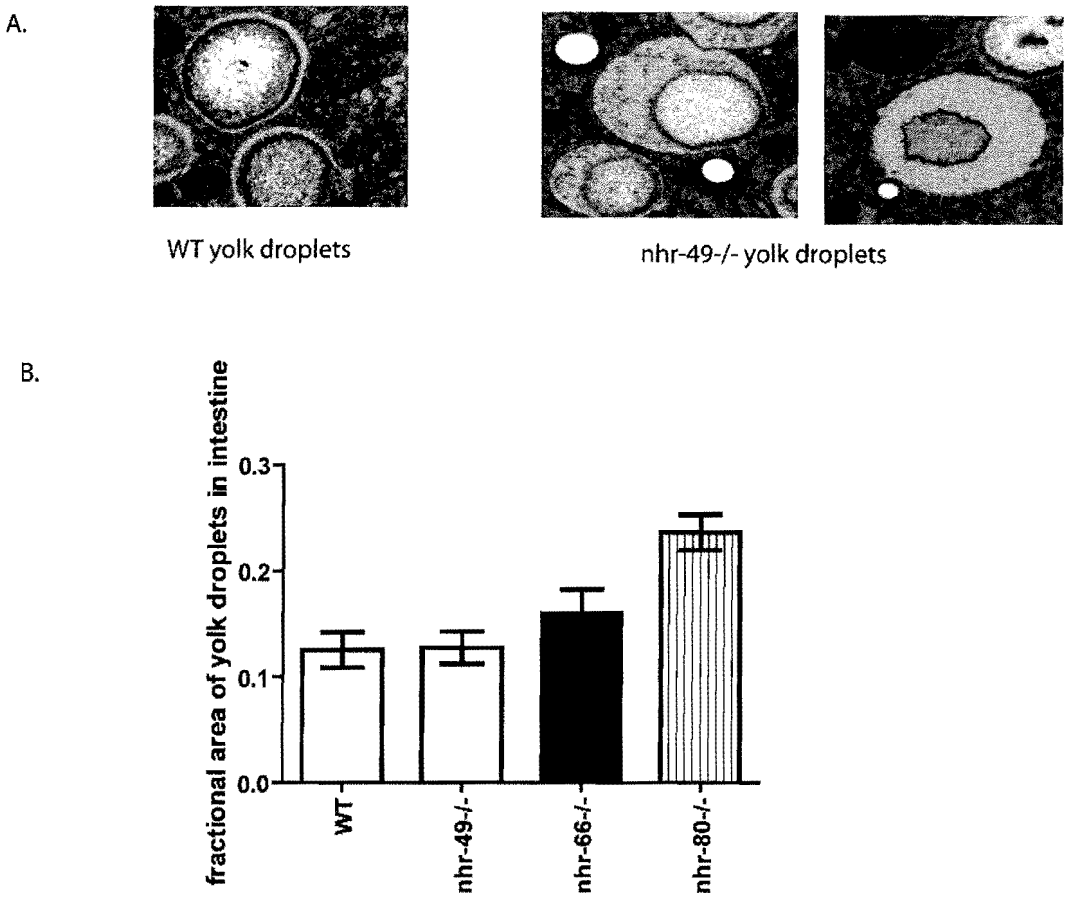

Fig 3.2. Quantification of yolk droplets in *nhr-49-/-* and its partner co-factors in *C. elegans* intestine.
A. High pressure freezing transmission electron microscopy (HP-TEM) images of yolk droplets in WT and *nhr-49-/-* animals.
B. The bar graph represents the mean (+/-SEM) fractional area of yolk droplets in the intestine of WT (white bar), *nhr-49-/-* (grey bar), *nhr-66-/-* (black bar) and *nhr-80-/-* (vertical stripes bar) animals. Atleast two animals were examined per mutant strain. p-value is not significant between WT and *nhr-49-/-*.

Fig. 3.3

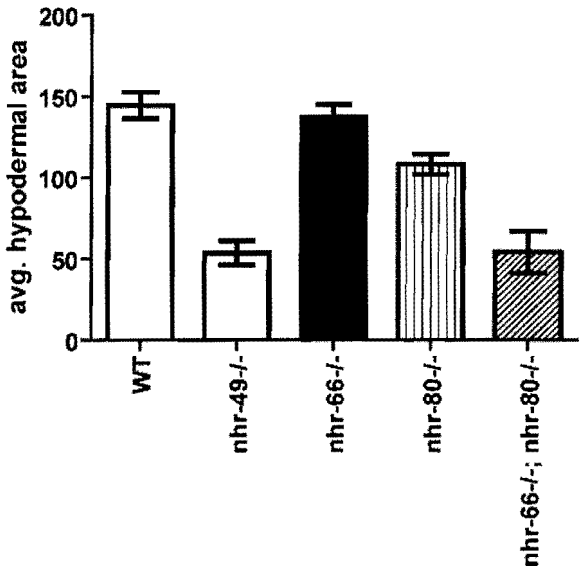

Fig. 3.3. Quantification of the size of hypodermis in *nhr-49-/-* and its partner co-factors.
The bar graph represents the mean (+/-SEM) fractional area of hypodermis area in the WT (white bar), *nhr-49-/-* (grey bar), *nhr-66-/-* (black bar), *nhr-80-/-* (vertical stripes bar) and *nhr-66-/-;nhr-80-/-* (slanted bar) animals. Atleast two animals were examined per mutant strain. p-value (compared to WT) < 0.005 (significant) for *nhr-49-/-* and *nhr-66-/-;nhr-80-/-*.

Fig. 3.4

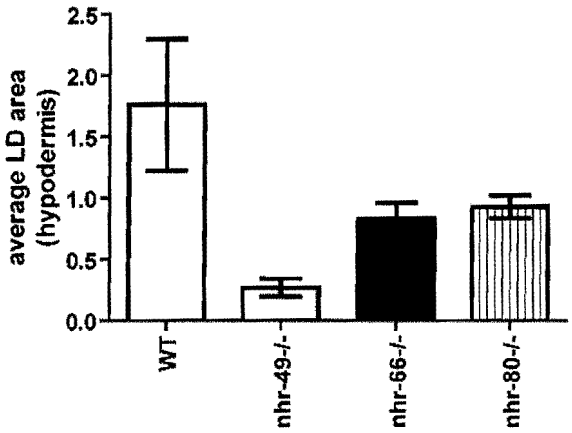

Fig. 3.4. Quantification of hypodermal lipid droplet size in *nhr-49-/-* and its partner co-factors.
The bar graph represents the mean (+/-SEM) hypodermal lipid droplet size in WT (white bar), *nhr-49-/-* (grey bar), *nhr-66-/-* (black bar) and *nhr-80-/-* (vertical stripes bar) animals. Atleast two animals were examined per mutant strain. p-value (compared to WT) < 0.05 (significant) for *nhr-49-/-*.

Fig 3.5

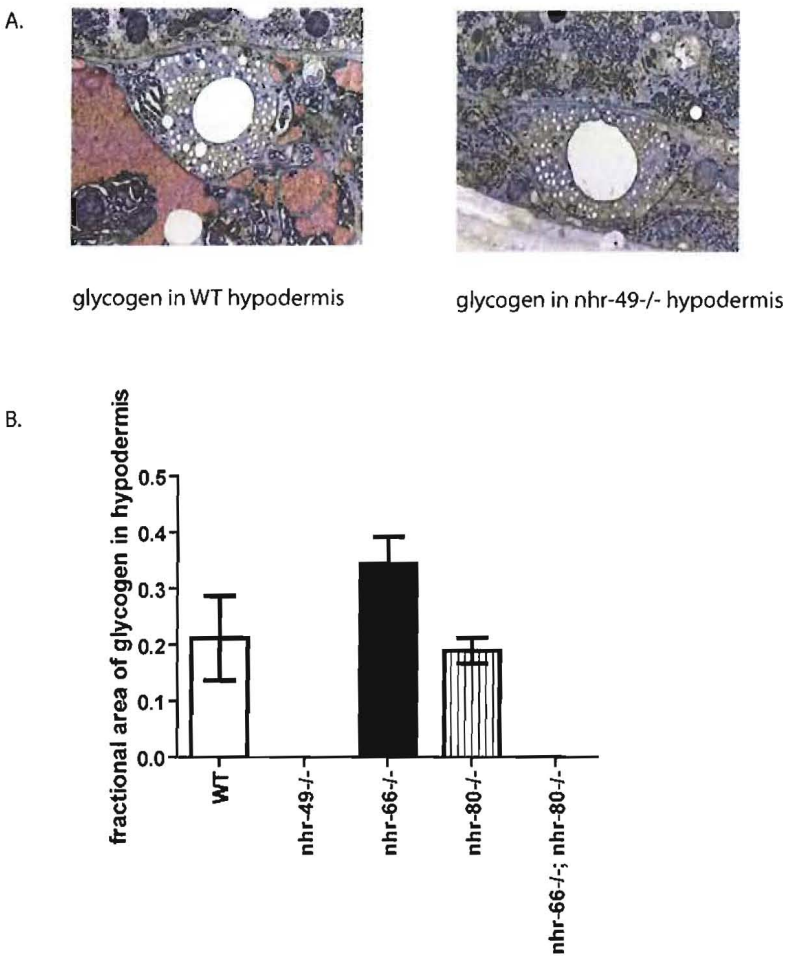

Fig. 3.5. Quantification of glycogen in *nhr-49-/-* and its partner co-factors in *C. elegans* hypodermis.
A. HP-TEM images of glycogen in the hypodermis of *wildtype* and *nhr-49-/-* animals. The region of the hypodermis containing glycogen has been digitally colored in red to highlight the difference between wildtype and *nhr-49-/-* glycogen levels.
B. The bar graph represents the mean (+/-SEM) fractional area of the glycogen in the hypodermis of WT (white bar), *nhr-49-/-* (grey bar), *nhr-66-/-* (black bar), *nhr-80-/-* (vertical stripes bar) and *nhr-66-/-;nhr-80-/-* (slanted bar) animals. Atleast two animals were examined per mutant strain.

Fig. 3.6

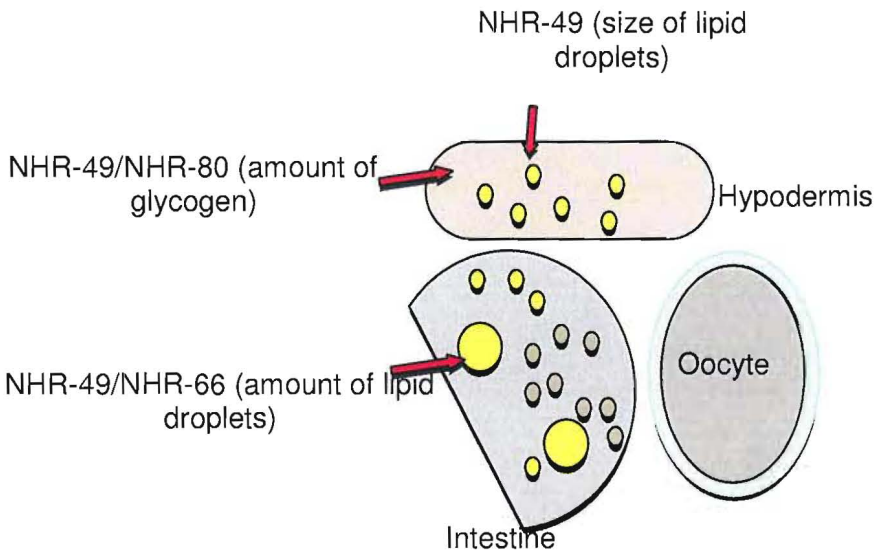

Fig. 3.6. Proposed model of NHR-49 and its co-factors in the regulation of different energy stores.
NHR-49 and NHR-66 regulate the amount of intestinal lipid droplets and NHR-49 and NHR-80 regulate the amount of hypodermal glycogen.

Fig. 3.7

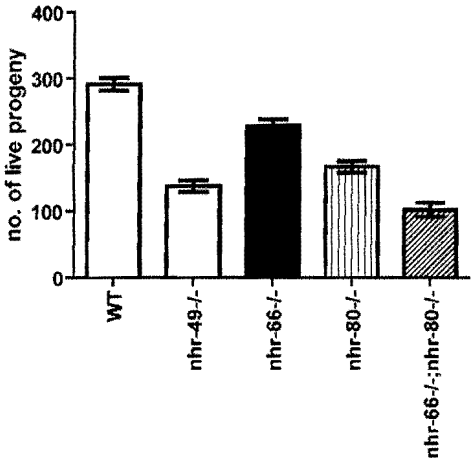

Fig 3.7. Brood size analysis of WT, *nhr-49-/-*, *nhr-66-/-* , *nhr-80-/-* and *nhr-66-/-;nhr-80-/-* animals.
The average number of progeny was the result of at least three independent experiments. p-value (compared to WT) < 0.0001 (significant) for *nhr-49-/-*, , *nhr-80-/-* and *nhr-66-/-;nhr-80-/-* and p-value (=0.0025) for nhr-66-/- (compared to WT)

Fig. 3.8

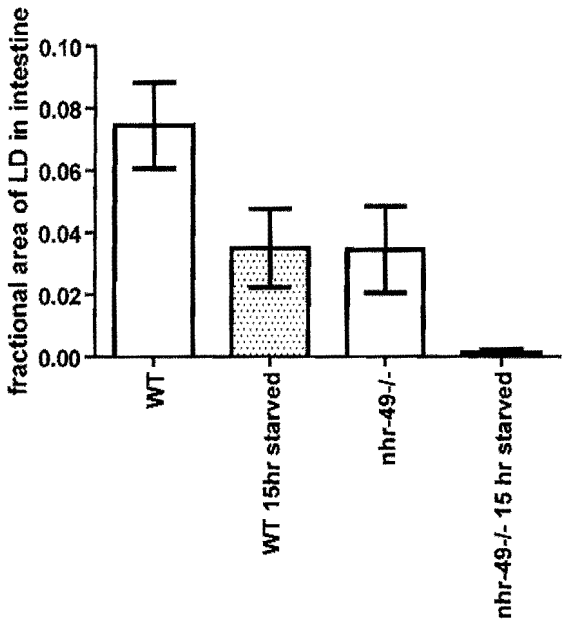

Fig. 3.8. Quantification of lipid droplets in 15 hour starved WT and *nhr-49-/- C. elegans* intestine.
The bar graph represents the mean (+/-SEM) fractional area of the intestinal lipid droplets of fed WT (white bar), starved WT (dotted white bar), fed *nhr-49-/-* (grey bar) and starved *nhr-49-/-* (dotted grey bar) animals. p-value < 0.05 (significant) compared between WT and WT 15 hr starved and p-value < 0.05 (significant) compared between *nhr-49-/-* and *nhr-49-/-* 15hr starved.

Fig. 3.9

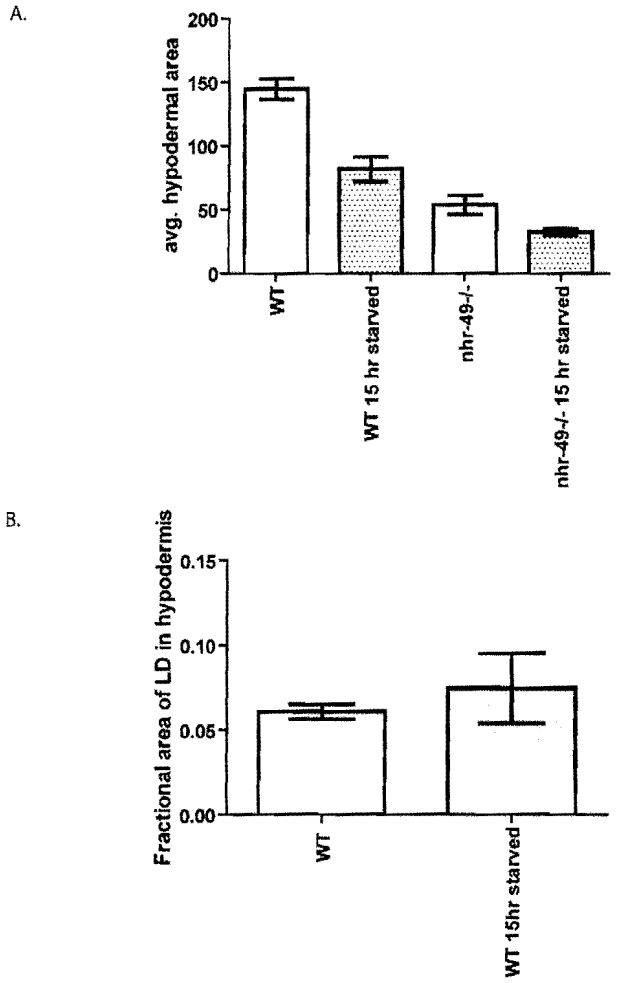

Fig. 3.9. Quantification of hypodermis size and fractional area of hypodermal lipid droplets in 15 hour starved WT and *nhr-49-/-* animals.
A. The bar graph represents the mean (+/-SEM) area of the hypodermis of fed WT (white bar), starved WT (dotted white bars), fed *nhr-49-/-* (grey bar) and starved *nhr-49-/-* (dotted grey bar) animals. p-value < 0.05 (significant) compared between WT and WT 15 hr starved and p-value < 0.05 (significant) compared between nhr-49-/- and *nhr-49-/-* 15hr starved.
B. The bar graph represents the mean (+/-SEM) fractional area of hypodermal lipid droplets of fed WT (white bar) and starved WT (grey bar) animals. p-value not significant between WT and WT 15 hr starved.

CHAPTER 4

ROLE OF NHR-49 IN MITOCHONDRIAL PHYSIOLOGY

Abstract

Nuclear receptor ligands that influence mitochondrial biogenesis and energy expenditure are popular compounds for promoting cardiovascular health, metabolic fitness, and overall wellbeing. The mitochondrial biogenic program involves the integration of several nuclear receptors that co-ordinate the expression of genes involved in multiple mitochondrial processes. We show that the *C. elegans* lipid sensing nuclear receptor, NHR-49 targets similar metabolic pathways to modulate mitochondrial biogenesis in nematodes. Like its mammalian counterparts, NHR-49 orchestrates the regulation of several target genes in multiple lipid metabolism pathways by partnering with distinct binding receptors to modulate a specific suite of genes that when knocked out yields corresponding sets of phenotypes. One such *nhr-49* knockout phenotype that we observed is the significant alteration in intestinal mitochondrial number and morphology. This is primarily attributed to impaired expression of genes in the fatty acid desaturase and sphingolipid breakdown pathways. Additionally, we demonstrated that one of the fatty acid desaturase genes *fat-7* and one of the sphingolipid breakdown genes acid ceramidase contribute to the aberrant *nhr-49* mitochondrial phenotype. Our work shows the involvement of very specific genes in the nuclear receptor mediated control of mitochondrial number and shape, paving the way for a better understanding of the transcriptional regulation of mitochondrial biogenesis.

Introduction

Mammalian PPAR agonists hold a lot of promise in the quest for novel therapeutic approaches in managing diverse metabolic and physical conditions. Collectively PPARs play important roles in energy homeostasis and have been implicated in obesity-related metabolic diseases. PPARs regulate genes involved in lipid uptake, storage and metabolism thereby intimately connecting them to mitochondria (Desvergne and Wahli 1999). Accordingly, the abundance, morphology and functional properties of mitochondria need to be fine tuned to meet the appropriate energy demands of specific cell types (Hock and Kralli 2009). However, because of PPAR's impact on such a broad set of target genes, the influence of their individual genes on specific aspects of mitochondrial function and as a result on overall animal physiology is largely unknown. Therefore in spite of PPAR ligands being at the forefront of pharmacological treatments for the metabolic syndrome, the pleiotropic nature of their gene expression makes it challenging to modulate only "the desired" effects of mitochondrial properties.

One of the co-activators of PPARs is PGC-1α, which has been described as a nuclear factor critical for activation of genes required for mitochondrial biogenesis in cell culture and rodent skeletal muscle (Puigserver, Wu et al. 1998). However, even though no effect of PPARα or PPARα ligands on PGC-1 expression have yet been reported, given the central and common pathways of regulation and function of PPARα and PGC-1α in liver, it has been suggested that PPARs, primarily appreciated for their effects on lipid metabolism, may have a wider impact on mitochondrial biogenesis and function by acting as transcriptional regulators of PGC-1 co-activators (Hock and Kralli 2009). Regulatory mechanisms must provide for the induction of the broad mitochondrial gene set and at the same time also enable inductions of tissue and signal specific gene sets.

The *C. elegans* NHR-49 is a functional homolog of PPAR-α, regulating mostly similar metabolic pathways and physiological processes, targeting similar sets of genes and displaying a similar panel of phenotypes thus providing an excellent context for genetic and biological studies of PPAR-α function (Van Gilst, Hadjivassiliou et al. 2005).

We therefore decided to take advantage of *C. elegans* genetics and explore the role of NHR-49 on mitochondrial physiology.

Results

NHR-49 is important for normal mitochondrial physiology

Based on our earlier work (chapter 2), we had hypothesized that the imbalance of lipid saturation observed in *nhr-49-/-* mutants could potentially contribute to altered membranes in organelles like mitochondria. Furthermore, gene expression data from our lab revealed that in addition to genes involved in lipid metabolism, NHR-49 and its partners co-regulate distinct sets of genes that fall into other physiological categories including the control of mitochondrial morphology (unpublished data, Van Gilst lab). Also, since PPARs have already been established to influence mitochondria by regulating several lipid metabolism pathways, we decided to investigate NHR-49's role in mitochondrial physiology (Desvergne and Wahli 1999) (Evans, Barish et al. 2004).

High Pressure-Transmission Electron Microscopy (HP-TEM) revealed multiple morphological defects in the mitochondria of one day old adult *nhr-49 (nr2041)* mutants compared to wildtype worms (figure 4.1). First, the mitochondria of the *nhr-49-/-* mutants were uncharacteristically irregular in shape as seen in figures 4.1A and B. They appear to have a lot more turns as opposed to the more rounded wildtype mitochondria. Figure 4.1E shows quantitative analysis of 10 consecutive transverse sections per worm measuring the number of turns in the mitochondria reflecting deviation from roundness in *nhr-49-/-* mitochondria versus control wildtype animals. Second, the average size of the mitochondria in *nhr-49-/-* mutants was at least two times the size of wildtype intestinal mitochondria (figures 4.1A, B and F). Third, we found that the average fractional area occupied by mitochondria per total intestinal area in *nhr-49-/-* mutants was much higher than that in wildtype animals (figures 4.1G, H, K). Fourth, we found that the cristae in the *nhr-49-/-* mutants appear denser and are not as distinct as those seen in wildtype (figures 4.1A, B). Finally, we observed small vesicles associated with these abnormally shaped mitochondria that appeared to be budding off of them.

Taken together, these results suggested that day one *nhr-49-/-* animals had altered mitochondrial physiology compared to same aged wildtype animals as measured using serial HP-TEM images obtained from the intestine.

Alternatively, we also labeled mitochondria using mitotracker red and used confocal microscopy to observe intestinal mitochondria of one day old adult wildtype and *nhr-49* mutants. However, we did not discern any observable difference in mitochondrial size or number by this technique (data not shown), presumably because of the limitations of resolution of confocal microscopy.

Partner co-factors contribute to NHR-49's regulation of mitochondrial number and morphology

We next wanted to determine if NHR-49 partners (chapter 2), NHR-66 and NHR-80 were contributing to the abnormal NHR-49 mitochondrial features. So, using deletion mutants of each interacting NHR-49 partner, we wanted to determine the individual effects of the different co-factors on the phenotype of *nhr-49-/-* mutants. In one day old adult *nhr-66 (ok940)* mutants, the roundness of the mitochondrial membrane was comparable to that of wildtype animals (figure 4.1C). However, even though the amount of intestinal area occupied by the mitochondria was significantly higher than wildtype and similar to levels seen in *nhr-49-/-* mutants (figures 4.1I and K), the size of the mitochondria (fig. 4.1F) was similar to wildtype animals suggesting that NHR-66 might be contributing to the number of mitochondria.

In one day old adult *nhr-80 (tm1011)* mutants, the mitochondrial membranes were misshapen and not as rounded as wildtype mitochondria (figures 4.1D and E). However, the size and fractional area of the mitochondria in the *nhr-80-/-* mutants was comparable to that of wildtype mitochondria (figures 4.1D, F, J, K). Based on these observations, we hypothesized that NHR-80 is contributing to the roundness of the membrane, therefore regulating the morphology of the mitochondria.

To test this hypothesis, we examined intestinal mitochondria in one day old adult *nhr-66-/-; nhr-80-/-* double mutants and in contrast to the *nhr-66-/-* and *nhr-80-/-* single deletion mutants, these double mutants had highly irregular shaped mitochondria (figures 4.2A and B), as was observed in the *nhr-49-/-* mutants. Thus, one possible explanation for the morphological abnormalities seen in *nhr-49-/-* mutants could be a combined effect of the misregulation of NHR-80 target genes (like fatty acid desaturases) and NHR-66 target genes (like enzymes involved in sphingolipid breakdown pathway).

Fatty acid desaturase contribute to mitochondrial morphology

We next tested the hypothesis that reduction in fatty acid desaturase expression was contributing to mitochondrial shape and examined wildtype animals on *fat-7 RNAi*. Just like we predicted, these animals displayed misshapen mitochondria (figures 4.3A and B). This supports the idea that fatty acid desaturases might be contributing to the shape of the mitochondrial membrane.

Ceramide implicated to play a role in mitochondrial number

To determine the potential NHR-66 regulated target genes that might be contributing to the increase in mitochondrial number, we evaluated knockouts of the different NHR-66 target genes in an *nhr-49-/-* background to see if any of them could suppress this mitochondrial phenotype. Indeed, the average fractional area occupied by mitochondria per total intestinal area in *nhr-49-/-;AC-/-* double mutants was significantly less than that of *nhr-49-/-* animals and appeared to be rescued to wildtype levels (figures 4.4A, B, C and D). Acid ceramidase breaks down ceramide to sphingosine. Thus, it is possible that the sphingolipid breakdown product, ceramide might be either playing a role in regulating mitochondrial biogenesis or promoting mitochondrial autophagy.

Discussion

Taken together, our data suggest that NHR-49 plays a previously unknown role in regulating mitochondrial physiology. We not only demonstrate that this involvement is due in part to NHR-49's regulation of its sphingolipid breakdown and fatty acid desaturase genes but also narrow it down to very specific genes in these two pathways (figure 4.5). This finding has important implications in the development of better therapeutic treatments that can eliminate detrimental side-effects.

Our data shows that *nhr-49-/-* mutants differ from wildtype animals in the size, number and shape of their intestinal mitochondria. It is known that NHR-49 and the PPARs (especially PPAR alpha and PPAR delta) influence similar genes in multiple lipid metabolism pathways, including fatty acid beta-oxidation and fatty acid desaturation. Like NHR-49, PPARs have also been implicated in regulating the density (number) of mitochondria. Indeed, PPAR gamma and PPAR delta have been shown to promote mitochondrial biogenesis in a cell-type specific manner. Treatment with PPAR gamma ligand pioglitazone in white adipose tissue and activation of PPAR delta in skeletal muscle both result in increased mitochondrial biogenesis (Tanaka, Yamamoto et al. 2003; Bogacka, Xie et al. 2005). However, in contrast to our data where *nhr-49-/-* mutants have mitochondria that are both uncharacteristically irregular in shape and are at least two times the size of wildtype mitochondria, the effects of PPARs on these two aspects of mitochondrial physiology are not yet known. One possibility is that like *nhr-49-/-* mutants, the different PPAR -/- mutants indeed display aberrant mitochondria but this has simply not been observed yet. It is also plausible that a set of genes not overlapping or common to NHR-49 and PPAR are contributing to the size and morphology of the mitochondria. In fact, our study revealed novel targets of NHR-49, mainly those involved in membrane lipid metabolism, particularly glycosphingolipid processing (chapter 2). Strikingly, a connection has not yet been reported for the role of PPARs in regulating sphingolipid metabolism in mammalian studies. PPARs however have been shown to influence mitochondrial function by mostly regulating genes encoding

mitochondrial fatty acid beta-oxidation enzymes and mitochondrial uncouplers (Puigserver, Wu et al. 1998).

Our EM analysis revealed that NHR-66 and NHR-80 are the regulatory modules contributing to the aberrant mitochondrial number and shape observed in *nhr-49-/-* mutants. NHR-49 interacts with NHR-66 to repress the expression of genes in the sphingolipid pathway whose breakdown products could be important mediators for maintaining the appropriate mitochondrial physiology as both *nhr-49-/-* and *nhr-66-/-* display an increase in mitochondrial number. Interestingly, in spite of the observed increase in mitochondrial number, we did not see any increase in the expression of mitochondrial gene transcripts. Specifically, our rescue experiments with *nhr-49-/-; AC-/-* double mutants demonstrate the significance of acid ceramidase in suppressing the altered mitochondrial density. On the other hand, NHR-49 together with NHR-80 facilitates the conversion of saturated fatty acids to monounsaturated fatty acids, and consequently, both *nhr-49-/-* and *nhr-80-/-* mutants are high in saturated fat and low in monounsaturated fat. This skewed ratio between saturated and unsaturated fat is likely the reason for the altered mitochondrial membrane "roundness" seen in *nhr-80-/-* and *nhr-49-/-* mutants. Since monounsaturated fatty acids are substrates for phospholipids, it is also possible that the misshapen mitochondrial membrane could be a result of improper phospholipid composition. Specifically, when animals were placed on *fat-7* RNAi we see an alteration in mitochondrial shape. Together, our results indicate that NHR-49 regulates mitochondrial number and morphology by regulating genes involved in sphingolipid breakdown and fatty acid desaturase pathways.

Based on our findings, we propose that ceramide plays a role in mitogenesis, whereas the desaturase gene *fat-7* impacts the mitochondrial membrane. We can further test this hypothesis by observing the fractional area of intestinal mitochondria in other players downstream of ceramide in the sphingolipid breakdown pathway, like sphingosine-phosphate lyase in an *nhr-49* background. Although we have not yet determined the mechanism by which ceramide might contribute to healthy mitochondria, we present several possibilities. Our favored hypothesis is that ceramide might be playing

a role in mitochondrial biogenesis. Hickson-Bick *et al* confirmed that in adult cardiomyocytes, ceramide stimulates apoptosis, whereas in fetal cardiomyocytes ceramide induces mitochondrial biogenesis (Hickson-Bick, Jones et al. 2008). Another possibility is that if the mitochondrial phenotype observed in *nhr-49-/-* mutants is partly due to a fission-fusion defect, there is considerable evidence in the literature that implicates ceramides in promoting fission and thus affecting mitochondrial dynamics. Strikingly, another recent publication demonstrated that during starvation, autophagosomes originate from mitochondrial outermembranes utilizing a mitochondrial lipid phosphatidylethanolamine that is conjugated to autophagosome markers (Hailey, Rambold et al. 2010). The suppression of phenotypes that we observe in the *nhr-49-/-; AC-/-* double mutants might be a result of modulation of phosphatidylethanolamine levels which is downstream of ceramide in the sphingolipid breakdown pathway.

Our finding that NHR-49 is a key regulator of mitochondrial physiology in *C. elegans* represents a considerable advance in our understanding of transcriptional regulation of mitochondrial biogenesis and function. As the global role of NHR-49 in the control of mitochondrial metabolism seems to be conserved, our findings could be envisaged as aiding in efforts to modulate specific target genes as opposed to a general manipulation of all the subsets of genes in that pathway.

Materials and methods

Nematode strains and growth conditions

C. elegans strains N2-Bristol (wildtype), *nhr-49* (2041), *nhr-66* (ok940), *nhr-80* (tm1011), *nhr-66-/-;nhr-80-/-* and *nhr-49-/-;AC-/-* were used for all experiments. Worms were maintained by standard techniques at 20°C. Single-worm PCR was used to determine the genotype of worms during crossing to generate *nhr-66-/-; 80-/-* and *nhr-49-/-;AC-/-* double-mutant lines.

High Pressure Transmission Electron microscopy

Day 1 adults were placed into a 20% BSA/PBS buffer solution and prepared in a Leica-Impact-2 high-pressure freezer according to the following protocol: 1) 60 hours in 100% acetone and uranyl acetate at –90°C. 2) Temperature was ramped from –90°C to –25°C over the course of 32.5 hours. 3) Next, sample was incubated at –25°C for 13 hours. 4) Next, the temperature change was brought from –25°C to 27°C in a 13 hour temperature ramp. Serial sections were post-stained in uranyl acetate followed by lead citrate. Thin cross sections were taken from resin-embedded clusters of young adults. Sections for adult animals were obtained from 3 different animals.

Quantification of mitochondria

Ten micron transverse sections typically spanning the length of the worm from the pharynx to the embryos were examined per animal. Mitochondria from each section were individually outlined and the average measurements were obtained using Image J software. Atleast two animals were examined per mutant strain.

Mitotracker staining

NGM 6cm plates were seeded with OP50 containing a final concentration of 500nM mitotracker Red. Animals at *L4* stage of development were placed on these plates in the dark at room temperature. Worms were mounted in a 2% agarose pad in M9 buffer containing sodium azide and then observed under a confocal microscope (Zeiss LSM 510 Meta). Pictures were taken by Zeiss LSM Imaging software at 40X and analyzed by Volocity V4.0 software.

Fig. 4.1

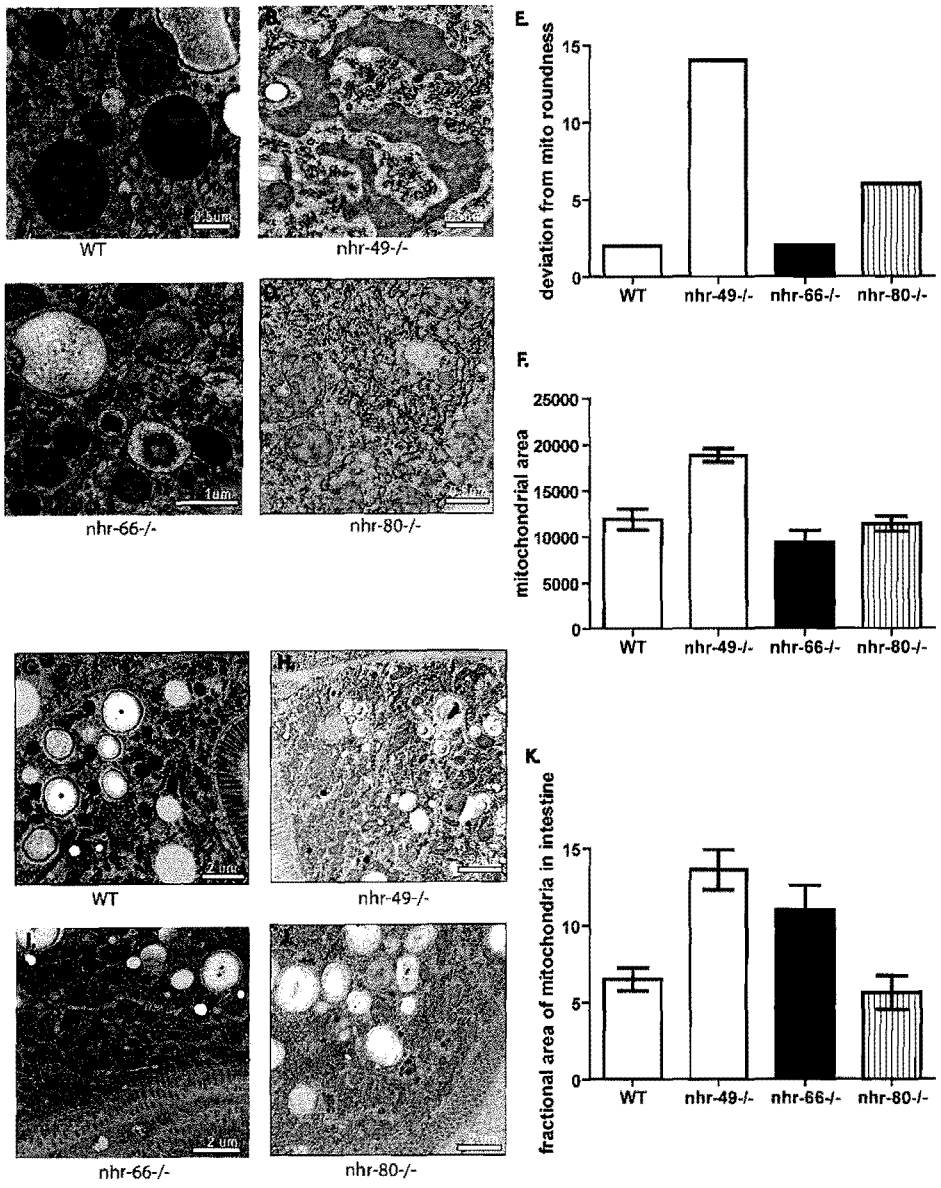
WT
nhr-49-/-
nhr-66-/-
nhr-80-/-
E
deviation from mito roundness
15
10
5
0
WT
nhr-49-/-
nhr-66-/-
nhr-80-/-
F
mitochondrial area
25000
20000
15000
10000
5000
0
WT
nhr-49-/-
nhr-66-/-
nhr-80-/-
WT
nhr-49-/-
nhr-66-/-
nhr-80-/-
K
fractional area of mitochondria in intestine
15
10
5
0
WT
nhr-49-/-
nhr-66-/-
nhr-80-/-

Fig. 4.2

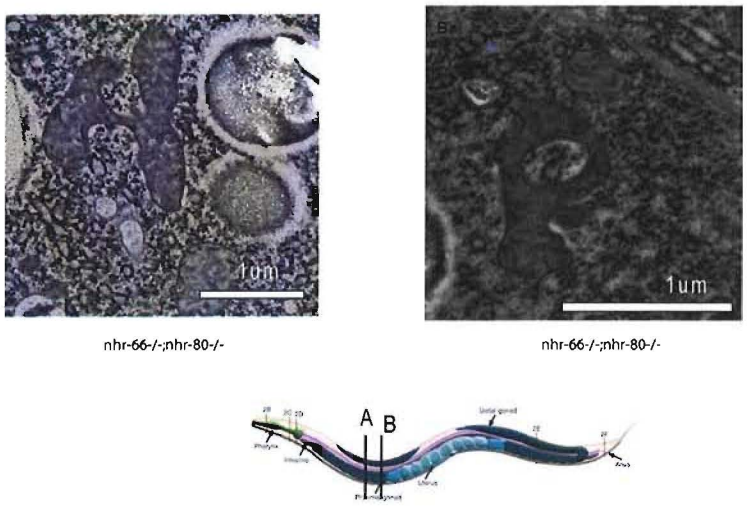

Fig. 4.2. HP-TEM images of *nhr-66-/-; nhr-80-/-* double mutants. Panel A and B corresponds to sections obtained from locations A and B highlighted in the worm schematic. Atleast three animals were examined.

Fig. 4.3

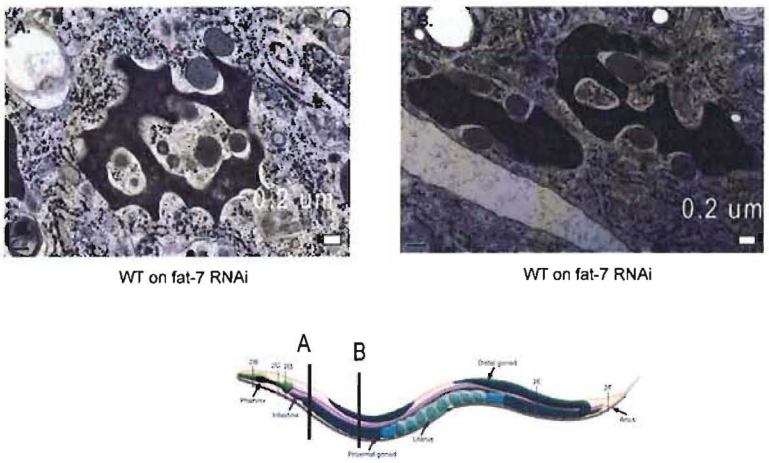

Fig. 4.3. HP-TEM images of wildtype on *fat-7* RNAi.
Panel A and B corresponds to sections obtained from locations A and B highlighted in the worm schematic.

Fig. 4.4

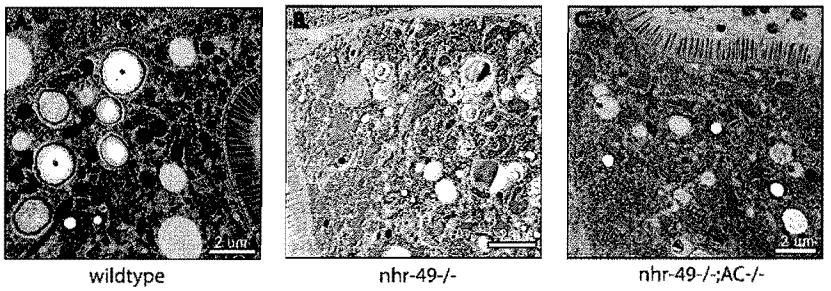

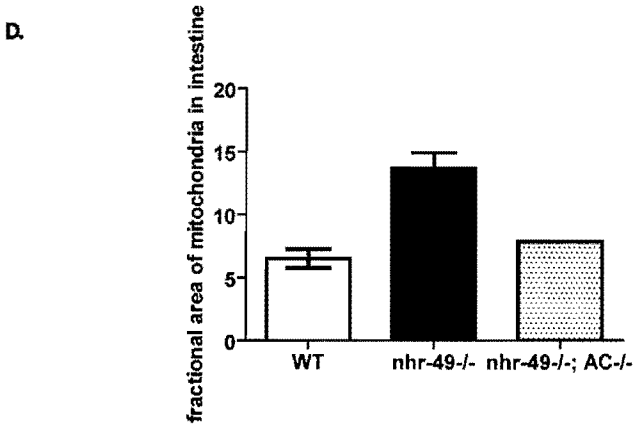

Fig. 4.4. Knockout of acid ceramidase (AC) in an *nhr-49* background rescues the aberrant *nhr-49-/-* mitochondrial phenotype.
A, B, C. HP-TEM image of N2, *nhr-49-/-* and *nhr-49-/-, AC-/-* mutants at the same magnification.
D. The bar graph represents the mean (+/-SEM) cross-sectional area in WT (white bars), *nhr-49-/-* (grey bars) and *nhr-49-/-, AC-/-* mutants (dotted bars).
Atleast two animals were examined per strain.

Fig. 4.5

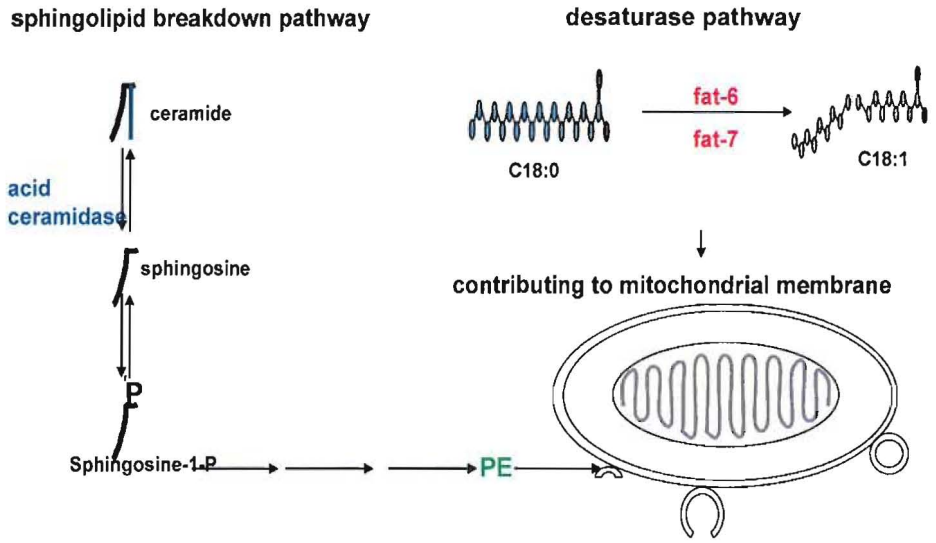

Fig. 4.6. Proposed model of NHR-49's influence on mitochondria physiology. Our data suggests that the desaturase pathway contributes to the shape and the sphingolipid pathway might be contributing to the number of mitochondria.

CHAPTER 5

CONCLUSIONS AND PERSPECTIVES

In this dissertation, I have presented a detailed characterization of the physiological role of NHR-49 in coordinating the multiple factors involved in maintaining the global homeostasis of lipid metabolism in *C. elegans*. In general, my work has contributed to a more complete picture of the extent to what nuclear receptors are capable of doing. This information is especially relevant as the technical limitations of mammalian studies make it difficult to address the gap in knowledge that exists between transcriptional regulation analyses and physiological phenotype studies. Compiling together the different findings that I have discovered from studying *C. elegans* NHR-49 contributes to a better understanding of the global impact of nuclear receptor regulated transcription on different aspects of animal physiology. Collectively, my work demonstrates that distinct aspects of NHR-49's overall impact, are executed by the orchestration of distinct metabolic pathways that together work to support NHR-49's overall function. These findings can complement and contribute to studies on mammalian nuclear receptor physiology as using *C. elegans* gives us the advantage of being able to identify genes and pathways and dissect complicated regulatory circuits, that otherwise would be difficult to do. Below, I highlight the significant findings of my work and speculate on future research.

Chapter 2: I demonstrated a co-ordinate regulation of lipid metabolism by a novel nuclear receptor partnership

I identified genes and pathways that are globally regulated by NHR-49. Based on binding data and gene expression analysis, I further identified three other nuclear receptors that serve as co-factors for NHR-49. These co-factors regulate very specific subsets of NHR-49's comprehensive gene targets. Even though I have demonstrated that NHR-49 can directly bind to NHR-66, NHR-80 and NHR-13 *in vitro*, it has not yet been determined if the different target genes are direct transcriptional targets and future work

using either gel shift assays or chromatin immunoprecipitation can be used to address this question. In addition, GFP-tagged constructs of NHR-49/NHR-66 and NHR-49/ NHR-80/ NHR-13 regulated genes will be useful in determining if there is overlapping tissue localization.

I used the deletion mutants of the different co-factors to parse out the contributions of distinct target genes on specific *nhr-49-/-* phenotypes. Since NHR-49 and PPARs are clearly regulating similar physiological processes and gene networks, this work is significant in understanding the physiological purpose and effects of the different target genes, especially in the context of designing therapeutic drugs with minimal side-effects. In addition, since the comprehensive list of different co-regulators involved in the HNF4α and PPAR transcriptional networks is not known, identifying and studying the impact of *C. elegans* NHR-49 co-factors is an important advancement. Even though it can be argued that the nematode NHR-66, NHR-80 and NHR-13 do not have any clear mammalian orthologs, this work suggests that there likely exist other mammalian co-factors that might function to regulate similar processes and pathways.

Finally, one of the outstanding questions in nuclear receptor biology is the significance of *C. elegans* having such an abundant number of nuclear receptors compared to say *Drosophila* or mammals. Specifically, evolutionary studies suggest that the ancestral HNF4 underwent a massive gene duplication event resulting in 269 family members (Robinson-Rechavi et al., 2005). One of the implications of this occurrence is that expansion could have allowed for worms to divide the different HNF4 functions and "outsource" them to different receptors. Alternatively, expansion could have allowed these receptors to evolve additional novel functions. This data thus provides new insights into the evolution of *C. elegans* nuclear receptor family. When I compare my findings of the *C. elegans* NHR-49 with other HNF-4-like nuclear receptors across species from yeast to mammals, a common theme that emerges is the conservation of its role in lipid metabolism pathways all throughout evolution. It can be speculated that the ancestral role of HNF-4 was most likely adopted by PPAR-α to primarily include mobilization of stored

energy during nutrient deprivation and the regulation of beta-oxidation, while the other functions of HNF-4 were either retained or outsourced to additional nuclear receptors.

Chapter 3: We identified a novel role for NHR-49 in the regulation of total energy stores and the subsequent influence on reproduction

It is not known how different transcriptional programs influence nuclear receptors to co-ordinate the distribution and delivery of fatty acids and sugars from and to multiple tissues, for the desired physiological demand under the relevant environmental condition. This question is technically difficult to address in mammalian systems. I used HP-TEM to illustrate that *C. elegans* NHR-49 and its co-factors are important players in the regulation of nutrient stores in the intestine and hypodermis. While a number of loss of function mutations and RNAi knockdowns have been reported that alter *C. elegans* lipid content and composition, the molecular mechanisms that regulate or affect lipid droplet fat stores or hypodermal glycogen stores are completely unknown. Even though further work is needed to identify the genes and other molecular players contributing to this regulation, I have demonstrated for the first time the influence of nuclear receptors in maintaining normal levels of lipid and glycogen stores in the intestine and hypodermis. In addition, I have been able to parse out the contribution of different co-factors NHR-66 and NHR-80 to this regulation. Given that the basic aspects of lipid metabolism have been shown to be conserved in mammals and worms, I speculate that our findings might also be relevant for mammalian nuclear receptors like PPARs.

My data also showed a strong correlation between reduced energy stores and compromised reproductive output. I showed that *nhr-49-/-* animals have a significantly reduced brood size and reduced mitotic region in the germline compared to wildtype controls. Future studies examining downstream effects on other organs can improve our understanding of the effect of energy stores on tissue function. Taken together, I postulate that NHR-49 could potentially act as a sensor for nutrient stores and accordingly adjust the physiological output. This hypothesis obviously needs to be tested further, but this is

a potentially exciting new framework to start thinking of the function nuclear receptors might be playing in coordinating "the supply and demand" of multiple types of nutrients to and from diverse locations in a "lipid economy" of the individual organism.

And lastly, even though *C. elegans* has historically been a great model for studying fat storage and fat metabolism, recent controversy over the current tools used to measure fat storage has come under considerable fire. Lipophilic dyes like Nile Red have been utilized to not only characterize fat storage but to also screen for novel regulators of fat storage; however a series of recent studies have shown that this dye primarily stains lysosome-related organelles which are not the primary fat storage sites in *C. elegans* (Yen, Le et al. 2010) (O'Rourke, Soukas et al. 2009). My study using high-pressure electron microscopy has revealed that there are typically two types of lipid containing vesicles: mono-layered lipid droplets located in the intestine and the hypodermis and multi-layered vesicles yolk droplets found in the intestine. Also, Nile Red does not stain the hypodermis, which our study reveals to contain lipid droplets. This work suggests that using ultrastructural analysis might be a better alternative to evaluating fat storage by Nile Red as it provides a snapshot of total lipid dynamics in the whole animal.

Chapter 4: We identified a previously unknown role for NHR-49 in mitochondrial physiology

I showed that NHR-49 plays a critical role in the regulation of *C. elegans* mitochondrial physiology. Ultrastructural studies revealed that *nhr-49-/-* animals had higher fractional area of intestinal mitochondria compared to controls. This is consistent with reports in mammalian PPARs where they have been shown to influence the number of mitochondria in a tissue-specific manner (Tanaka, Yamamoto et al. 2003; Bogacka, Xie et al. 2005). In this study, I have primarily focused on the *C. elegans* intestine and it will be interesting to see what future studies will reveal in other tissues like hypodermis and muscle. Additionally, *nhr-49-/-* animals also had misshapen intestinal mitochondria compared to wildtype animals. To date, there have been no studies reporting nuclear receptor mediated effects on mitochondria shape. It could be plausible that the different

PPAR -/- mutants indeed display aberrant mitochondria but they have not yet been observed.

I used deletion mutants to separate out these *nhr-49-/-* phenotypes and identified the NHR-49 regulated pathways responsible for the alteration of mitochondrial shape and number. Specifically, my data suggested that NHR-66 together with NHR-49 regulated mitochondrial number and NHR-49 together with NHR-80 regulated mitochondrial shape. Furthermore, I identified the individual genes in these metabolic pathways that might be contributing to these effects. Since all the target genes of the PPAR transcriptional network are not completely known, it is possible that a set of genes not overlapping or common to NHR-49 and PPAR are contributing to the size and morphology of the mitochondria. In fact, this study revealed novel targets of NHR-49, mainly those involved in sphingolipid processing and lipid remodeling. Strikingly, a connection has not yet been reported for the role of PPARs in regulating sphingolipid metabolism in mammalian studies. PPARs however have been shown to influence mitochondrial function by mostly regulating genes encoding mitochondrial fatty acid beta-oxidation enzymes and mitochondrial uncouplers

Although further studies are needed to determine the molecular mechanisms that are responsible for the mitochondrial effects, my findings so far are still significant in the field especially because mammalian PPARs are known to broadly regulate an extensive set of target genes, but the specific influence of individual genes on distinct facets of mitochondrial function have not been delineated and therefore poorly understood. Since many of the components that are central to governing human metabolism are conserved in worms, our findings will definitely add to ongoing mammalian studies.

REFERENCES

Ashrafi, K., F. Y. Chang, et al. (2003). "Genome-wide RNAi analysis of Caenorhabditis elegans fat regulatory genes." Nature **421**(6920): 268-272.

Bertrand, S., F. G. Brunet, et al. (2004). "Evolutionary Genomics of Nuclear Receptors: From Twenty-Five Ancestral Genes to Derived Endocrine Systems." Molecular Biology and Evolution **21**(10): 1923-1937.

Bogacka, I., H. Xie, et al. (2005). "Pioglitazone Induces Mitochondrial Biogenesis in Human Subcutaneous Adipose Tissue In Vivo." Diabetes 54(5): 1392-1399.

Chawla, A., J. J. Repa, et al. (2001). "Nuclear receptors and lipid physiology: opening the X-files." Science **294**(5548): 1866-1870.

Consortium, T. C. e. S. (1998). "Genome Sequence of the Nematode C. elegans: A Platform for Investigating Biology." Science **282**(5396): 2012-2018.

Desvergne, B. and W. Wahli (1999). "Peroxisome proliferator-activated receptors: nuclear control of metabolism." Endocr Rev **20**(5): 649-688.

Dhe-Paganon, S., K. Duda, et al. (2002). "Crystal Structure of the HNF4α Ligand Binding Domain in Complex with Endogenous Fatty Acid Ligand." Journal of Biological Chemistry **277**(41): 37973-37976.

Desvergne, B. and W. Wahli (1999). "Peroxisome Proliferator-Activated Receptors: Nuclear Control of Metabolism." Endocr Rev 20(5): 649-688.

Evans, R. M., G. D. Barish, et al. (2004). "PPARs and the complex journey to obesity." Nat Med 10(4): 355-361.

Glass, C. K. and M. G. Rosenfeld (2000). "The coregulator exchange in transcriptional functions of nuclear receptors." Genes & Development **14**(2): 121-141.

Gupta, R. K., N. Gao, et al. (2007). "Expansion of adult beta-cell mass in response to increased metabolic demand is dependent on HNF-4{alpha}." Genes & Development **21**(7): 756-769.

Hayhurst, G. P., Y.-H. Lee, et al. (2001). "Hepatocyte Nuclear Factor 4{alpha} (Nuclear Receptor 2A1) Is Essential for Maintenance of Hepatic Gene Expression and Lipid Homeostasis." Molecular and Cellular Biology **21**(4): 1393-1403.

Hailey, D. W., A. S. Rambold, et al. (2010). "Mitochondria supply membranes for autophagosome biogenesis during starvation." Cell 141(4): 656-667.

Hickson-Bick, D. L., C. Jones, et al. (2008). "Stimulation of mitochondrial biogenesis and autophagy by lipopolysaccharide in the neonatal rat cardiomyocyte protects against programmed cell death." J Mol Cell Cardiol 44(2): 411-418.

Hock, M. B. and A. Kralli (2009). "Transcriptional Control of Mitochondrial Biogenesis and Function." Annual Review of Physiology 71: 177-203.

Jones, K. T. and K. Ashrafi (2009). "Caenorhabditis elegans as an emerging model for studying the basic biology of obesity." Disease Models & Mechanisms **2**(5-6): 224-229.

Jones, K. T., E. R. Greer, et al. (2009). "<italic>Rictor</italic>/TORC2 Regulates <named-content xmlns:xlink="http://www.w3.org/1999/xlink" content-type="genus-species" xlink:type="simple">Caenorhabditis elegans</named-content> Fat Storage, Body Size, and Development through <italic>sgk-1</italic>." PLoS Biol **7**(3): e1000060.

Kersten, S., J. Seydoux, et al. (1999). "Peroxisome proliferator–activated receptor α mediates the adaptive response to fasting." The Journal of Clinical Investigation **103**(11): 1489-1498.

Leone, T. C., C. J. Weinheimer, et al. (1999). "A critical role for the peroxisome proliferator-activated receptor α (PPARα) in the cellular fasting response: The PPARα-null mouse as a model of fatty acid oxidation disorders." Proceedings of the National Academy of Sciences **96**(13): 7473-7478.

Liang, B., K. Ferguson, et al. (2010). "The Role of Nuclear Receptor NHR-64 in Fat Storage Regulation in <italic>Caenorhabditis elegans</italic>." PLoS One **5**(3): e9869.

Listenberger, L. L., X. Han, et al. (2003). "Triglyceride accumulation protects against fatty acid-induced lipotoxicity." Proceedings of the National Academy of Sciences **100**(6): 3077-3082.

Lucas, B., K. Grigo, et al. (2005). "HNF4[alpha] reduces proliferation of kidney cells and affects genes deregulated in renal cell carcinoma." Oncogene **24**(42): 6418-6431.

Magner, D. B. and A. Antebi (2008). "Caenorhabditis elegans nuclear receptors: insights into life traits." Trends in Endocrinology & Metabolism **19**(5): 153-160.

Miquerol, L., S. Lopez, et al. (1994). "Expression of the L-type pyruvate kinase gene and the hepatocyte nuclear factor 4 transcription factor in exocrine and endocrine pancreas." Journal of Biological Chemistry **269**(12): 8944-8951.

Naiki, T., M. Nagaki, et al. (2002). "Analysis of Gene Expression Profile Induced by Hepatocyte Nuclear Factor 4α in Hepatoma Cells Using an Oligonucleotide Microarray." Journal of Biological Chemistry **277**(16): 14011-14019.

Ntambi, J. M. (1995). "The regulation of stearoyl-CoA desaturase (SCD)." Progress in Lipid Research **34**(2): 139-150.

Odom, D. T., N. Zizlsperger, et al. (2004). "Control of Pancreas and Liver Gene Expression by HNF Transcription Factors." Science **303**(5662): 1378-1381.

O'Rourke, E. J., A. A. Soukas, et al. (2009). "C. elegans Major Fats Are Stored in Vesicles Distinct from Lysosome-Related Organelles." Cell Metabolism **10**(5): 430-435.

Palanker, L., J. M. Tennessen, et al. (2009). "Drosophila HNF4 Regulates Lipid Mobilization and [beta]-Oxidation." Cell Metabolism **9**(3): 228-239.

Parks, D. J., S. G. Blanchard, et al. (1999). "Bile Acids: Natural Ligands for an Orphan Nuclear Receptor." Science **284**(5418): 1365-1368.

Partridge, L., D. Gems, et al. (2005). "Sex and Death: What Is the Connection?" Cell **120**(4): 461-472.

Peet, D. J., B. A. Janowski, et al. (1998). "The LXRs: a new class of oxysterol receptors." Current Opinion in Genetics & Development **8**(5): 571-575.

Perissi, V. and M. G. Rosenfeld (2005). "Controlling nuclear receptors: the circular logic of cofactor cycles." Nat Rev Mol Cell Biol **6**(7): 542-554.

Peter, A., C. Weigert, et al. (2008). "Induction of stearoyl-CoA desaturase protects human arterial endothelial cells against lipotoxicity." American Journal of Physiology - Endocrinology And Metabolism **295**(2): E339-E349.

Phelps, C., V. Gburcik, et al. (2006). "Fungi and animals may share a common ancestor to nuclear receptors." Proceedings of the National Academy of Sciences **103**(18): 7077-7081.

Piper, M. D. W., D. Skorupa, et al. (2005). "Diet, metabolism and lifespan in Drosophila." Experimental Gerontology **40**(11): 857-862.

Porte, D., D. G. Baskin, et al. (2005). "Insulin Signaling in the Central Nervous System." Diabetes **54**(5): 1264-1276.

Puigserver, P., Z. Wu, et al. (1998). "A cold-inducible coactivator of nuclear receptors linked to adaptive thermogenesis." Cell 92(6): 829-839.

Rhodes, C. J. (2005). "Type 2 Diabetes-a Matter of {beta}-Cell Life and Death?" Science **307**(5708): 380-384.

Schaffer, J. E. (2003). "Lipotoxicity: when tissues overeat." Current Opinion in Lipidology **14**(3): 281-287.

Shimabukuro, M., M. Higa, et al. (1998). "Lipoapoptosis in Beta-cells of Obese Prediabeticfa/fa Rats." Journal of Biological Chemistry **273**(49): 32487-32490.

Sluder, A. E. and C. V. Maina (2001). "Nuclear receptors in nematodes: themes and variations." Trends in Genetics **17**(4): 206-213.

Sonoda, J., L. Pei, et al. (2008). "Nuclear receptors: Decoding metabolic disease." FEBS Letters **582**(1): 2-9.

Stoffel, M. and S. A. Duncan (1997). "The maturity-onset diabetes of the young (MODY1) transcription factor HNF4α regulates expression of genes required for glucose transport and metabolism." Proceedings of the National Academy of Sciences **94**(24): 13209-13214.

Tanaka, T., J. Yamamoto, et al. (2003). "Activation of peroxisome proliferator-activated receptor delta induces fatty acid beta-oxidation in skeletal muscle and attenuates metabolic syndrome." Proc Natl Acad Sci U S A 100(26): 15924-15929.

Taubert, S., M. R. Van Gilst, et al. (2006). "A Mediator subunit, MDT-15, integrates regulation of fatty acid metabolism by NHR-49-dependent and -independent pathways in C. elegans." Genes Dev **20**(9): 1137-1149.

Unger, R. H. and Y. T. Zhou (2001). "Lipotoxicity of beta-cells in obesity and in other causes of fatty acid spillover." Diabetes **50**(suppl 1): S118.

Van Gilst, M. R., H. Hadjivassiliou, et al. (2005). "Nuclear hormone receptor NHR-49 controls fat consumption and fatty acid composition in C. elegans." PLoS Biol **3**(2): e53.

Wang, Y.-X., C.-H. Lee, et al. (2003). "Peroxisome-Proliferator-Activated Receptor [delta] Activates Fat Metabolism to Prevent Obesity." Cell **113**(2): 159-170.

Watts, J. L. and J. Browse (2002). "Genetic dissection of polyunsaturated fatty acid synthesis in Caenorhabditis elegans." Proc Natl Acad Sci U S A **99**(9): 5854-5859.

Wymann, M. P. and R. Schneiter (2008). "Lipid signalling in disease." Nat Rev Mol Cell Biol **9**(2): 162-176.

Yamagata, K., H. Furuta, et al. (1996). "Mutations in the hepatocyte nuclear factor-4[alpha] gene in maturity-onset diabetes of the young (MODY1)." Nature **384**(6608): 458-460.

Yen, K., T. T. Le, et al. (2010). "A Comparative Study of Fat Storage Quantitation in Nematode <italic>Caenorhabditis elegans</italic> Using Label and Label-Free Methods." PLoS One **5**(9): e12810.

CURRICULUM VITAE

EDUCATION

September 2005-2011 **PhD** (Molecular and Cellular Biology)
University of Washington-Seattle

June 1998-May 2000 **M.S.** (Veterinary Science)
Animal Health and Biomedical Sciences
University of Wisconsin-Madison

July 1996-May 1998 **B.S.** (Genetics and Biochemistry)
College of Agriculture and Life sciences
University of Wisconsin-Madison

July 1994-May 1996 Life Sciences
Sophia College
University of Bombay-India

RESEARCH EXPERIENCE

September 2005-present **Graduate student, PhD Advisor: Dr. MarcVan Gilst, Fred Hutchinson Cancer Research Center, University of Washington-Seattle**

Characterizing NHR-49, the *C.elegans* homolog of the mammalian lipid sensing nuclear receptors

- Demonstrated a novel nuclear receptor partnership involved in the regulation of lipid metabolism by identifying three NHR-49 binding nuclear receptors with each partner protein accounting for a specific subset of NHR-49 target genes and corresponding phenotypes
- Identified a previously unknown role for NHR-49 in regulating mitochondrial physiology

November 2002-August 2005 Teaching Associate, Dr. Ted Gross, Department of Orthopedics, University of Washington-Seattle

Studying the cellular and molecular effects of bone cells exposed to hypoxia.

- Responsiblities included planning, designing and conducting *in vitro* bone cell hypoxia experiments, performing Western blot and RT-PCR analyses on cell extracts, performing histologic and immunohistochemical analysis on bone tissue, using FACS and cell death assays to look for apoptosis, using tissue culture to

maintain cell lines for different *in vitro* experiments and teaching and mentoring the above techniques to other laboratory employees.

October 2000-August 2002 Research Assistant II, Department of Research, Targeted Genetics Corporation

Generating, characterizing (physically and biologically) gene expression constructs and their incorporation into novel, targeted, lipid and polymer based gene delivery systems.

- Responsibilities included synthesis of LPD formulations for *in vitro* experiments, designing and analyzing *in vitro* transfection experiments, processing *in vivo* tissue samples, making gene constructs, assisting in assay development, using tissue culture to maintain cell lines for different *in vitro* and *in vivo* experiments.

June 1998-May 2000 Graduate student, Masters advisor: Dr. Judd M Aiken, Department of Animal Health and Biomedical Sciences, University of Wisconsin-Madison

Researched the impact of mitochondrial electron transport system (ETS) enzymatic activities on aging skeletal and cardiac muscles.

- Designed riboprobes to study the effect of mitochondrial ETS abnormalities on the RNA
  expression of selected genes.
- Demonstrated the presence of increased steady-state levels of oxidative nucleic acid damage in aged rat muscle fibers using immunohistochemical staining with an antibody specific for DNA and RNA oxidative damage.
- Elucidated the fate of ETS abnormal skeletal muscle fibers in different aged rats with markers of apoptosis using TUNEL to detect DNA fragmentation and immunohistochemistry to detect bcl-2 levels.

PRESENTATIONS AND PUBLICATIONS

Papers

1. **Pranali Pathare**, Marc Van Gilst. Co-ordinate regulation of lipid metabolism by a novel nuclear receptor partnership. (in preparation)

2. **Pranali Pathare**, Marc Van Gilst. Role of NHR-49 and its partners in energy distribution. (in preparation)

3. Ted Gross, Katy King, Natalia Rabaia, **Pranali Pathare**, Sundar Srinivasan. Upregulation of osteopontin by osteocytes deprived of mechanical loading or oxygen. JBMR. 20 (2), 250-256, '05.

4. Jonathan Wanagat, Zhenjin Cao, **Pranali Pathare**, Judd M. Aiken. Mitochondrial DNA deletion mutations colocalize with segmental electron transport system abnormalities, muscle fiber atrophy, fiber splitting, and oxidative damage in sarcopenia. FASEB J. 15, 322-332, '01.

Talks

1. **Pranali Pathare**, Marc Van Gilst. Co-ordinate regulation of sphingolipid metabolism by nuclear receptor partnership. International Worm Meeting. Los Angeles, CA, 2007.

2. **Pranali Pathare**, Marc Van Gilst. NHR-49: regulator of lipid metabolism. Seattle Worm Meeting. Seattle, WA, 2007.

Poster presentations and published abstracts

1. **Pranali Pathare**, Tessie Ng, Marc Van Gilst. NHR-49 influences mitochondrial physiology by regulating distinct aspects of lipid metabolism. Nuclear Receptor Meeting. Cold Spring Harbor, NY, 2010.

2. **Pranali Pathare**, Marc Van Gilst. Co-ordinate regulation of lipid metabolism by a novel nuclear receptor partnership. International Worm Meeting, Los Angeles, CA, 2009.

3. **Pranali Pathare**, Ted Gross. Heat shock protein modulation by hypoxic osteocytes. American Society of Bone and Mineral Research, Seattle, WA, 2004.

4. Jon Wanagat, Nate Van Zeeland, **Pranali Pathare**, Judd M. Aiken. Segmental mitochondrial abnormalities concurrent with skeletal muscle fiber oxidative damage, atrophy and splitting. American Aging Association Annual Meeting, Boston, MA, 2000.

5. Allen Herbst, Jon Wanagat, **Pranali Pathare**, Judd M. Aiken. Age-associated electron system abnormalities concurrent with intra-fiber atrophy in rat skeletal muscle fibers. American Aging Association Annual Meeting, Seattle, WA, 1999.

- Attended the Annual American Society of Gene Therapy (ASGT) Conference in Seattle, WA, 2001.

TEACHING EXPERIENCE

2007 Spring quarter	Teaching assistant, Cell Biology 355, Dr. Rose Ann Cattolico and Dr. Andrew Christie, University of Washington
2008 to 2009	Science Education Program